CHAPTER 6

Chemical Dynamics of Melts and Crystals

FUNDAMENTAL QUESTIONS CONSIDERED IN THIS CHAPTER

1. How do atomic-scale, time-dependent kinetic phenomena govern changing states of melts? How do melts flow as viscous liquids?
2. What is viscosity, what factors control the viscosity of melts, and how does viscosity impact the dynamic behavior of melts?
3. What is diffusion, what factors control rates of atomic and thermal diffusion, and how do these rates impact crystallization and vesiculation of melts?
4. How do crystals nucleate, grow, and modify their shape and size?
5. How do exsolved volatile bubbles nucleate, grow, and fragment melts?

INTRODUCTION

In dynamic magmatic systems, changing intensive parameters and energy conditions cause the state of the system to change, but only insofar as kinetic factors allow. Thus, the rate at which the *T* of a magma decreases is commonly faster than the rate at which kinetically controlled crystallization can progress, creating compositionally zoned crystals and reaction rims in the fractionating magma. Sluggish kinetic rates prevent homogenization of the zoned crystal and equilibration via reaction relations with the enclosing melt, even though temperatures may be relatively high. Instantaneous change from an initial metastable state to a new state of more stable, perfect equilibrium almost never takes place in magmatic systems because of slow kinetics.

In this chapter, we focus on kinetic factors that operate on the atomic level in controlling two basic dynamic aspects of melts—solidification and vesiculation-fragmentation. Whether the same granitic melt solidifies to a massive metastable glass; to an aphanitic or to a phaneritic aggregate of quartz, feldspar, and biotite crystals; to highly vesicular pumice; or to fine ash particles depends on the interplay between rates of changing environmental conditions, such as *T,* and kinetic (time-dependent) process rates. The nature of the kinetic history, or kinetic path, taken by the changing melt during solidification or vesiculation is recorded in the fabric of the resulting rock, discussed in the following chapter.

Section 3.6 introduced kinetic phenomena. A comprehensive treatment is Lasaga (1998).

The first three sections of this chapter deal with three so-called **transport phenomena** (Figure 6.1):

1. Transport of viscous material, sometimes referred to as a transfer of momentum (mass × velocity)
2. Transfer of atoms, usually referred to as chemical diffusion
3. Transfer of heat by conduction (Section 1.1.3)

Each of these three transport processes has a driving force and a proportionality constant that is an intrinsic property of the material. Each depends in some way on the movement of atoms.

❊6.1 VISCOSITY OF MELTS

On an atomic scale in melts, viscosity is a measure of the mobility of atoms, how readily atomic bonds can be stretched, broken, and reformed with neighboring

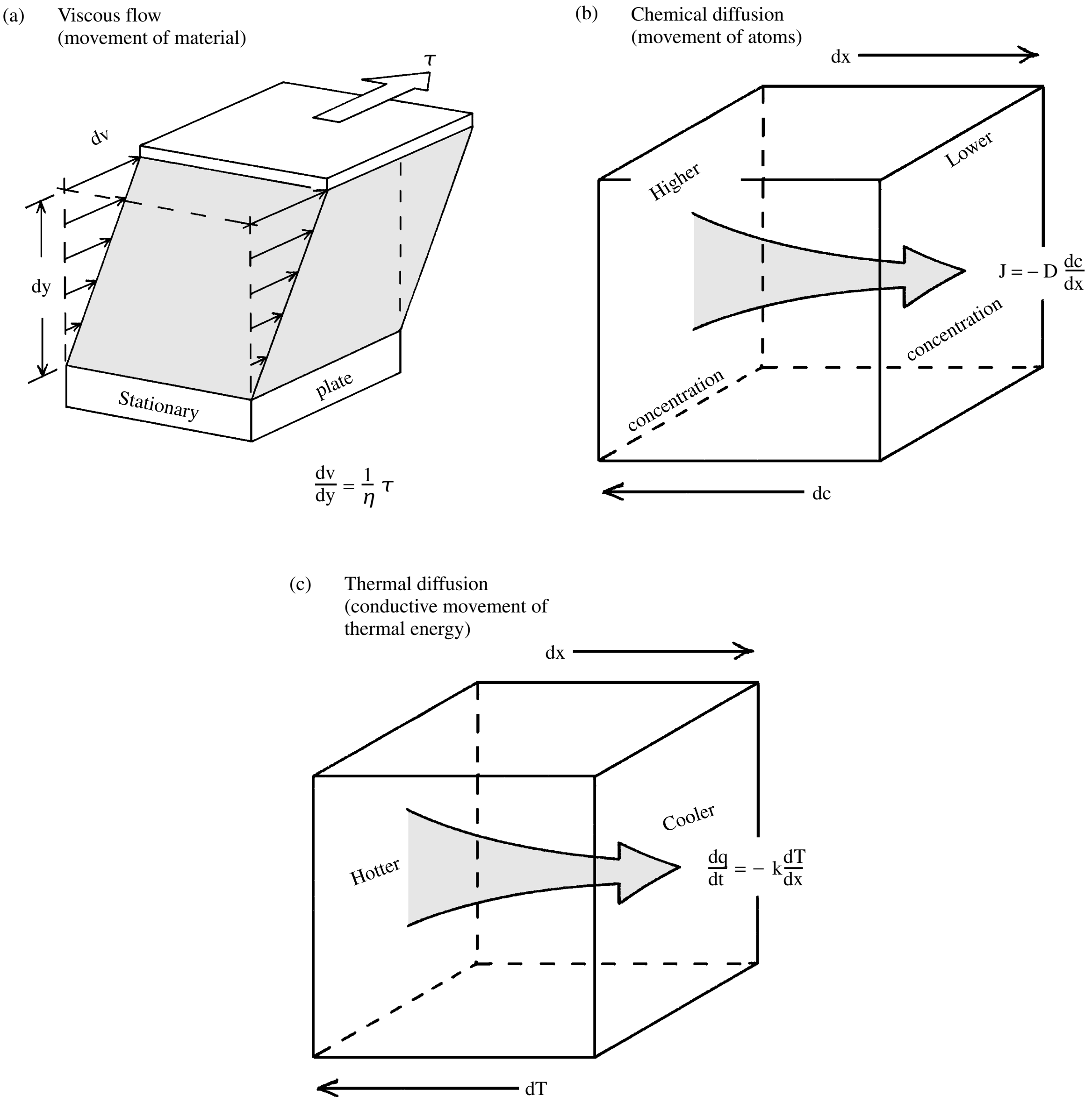

6.1 Three **transport phenomena.** All involve a gradient in some quantity that provides a driving force for transport and all follow similar laws. (a) **Viscous flow** in a cube of material (dashed lines) is driven by a force applied tangentially to its upper surface area. This applied shear stress (force/area = stress), τ, produces a change in the shape of the body so that the cube becomes a parallelepiped. The change in shape, called strain, ε, becomes more extreme with time, that is, the applied shear stress creates a certain strain rate, *dε/dt,* whose magnitude depends on the viscosity of the particular material, η. The strain rate is equivalent to a velocity gradient, *dv/dy,* which is shown by arrows of increasing length over the distance *dy.* (b) **Chemical diffusion** is driven by a change in concentration, *dc,* of some particular atoms between a region of higher concentration (left face of the cubical volume of material) and lower concentration (right face); these two faces are separated by a distance, *dx.* The concentration gradient, *dc/dx,* produces a flow of atoms, *J,* down the gradient. (c) **Thermal diffusion,** or **heat conduction,** is driven by a gradient in temperature over a distance, *dT/dx,* and produces a flow of heat over time, *dq/dt.* The proportionality constants for these three types of transport are intrinsic properties of the material. For viscous flow the constant is the coefficient of viscosity, or viscosity, η; for chemical diffusion it is the diffusion coefficient, or diffusivity, *D;* and for heat conduction it is the thermal conductivity, *k.*

atoms. Solidification of melts and exsolution of volatile components from them, which are the two principal themes of this chapter, involve the movement of atoms, or the lack thereof. The ease with which atoms can move about is expressed on a larger macroscopic scale in a body of material, such as a lava flow, in its resistance to flow or deformation. On both scales, **viscosity** is a manifestation of mobility. Less mobility corresponds to greater viscosity. "Fluidity" and viscosity are inversely related (opposites).

Unquestionably, viscosity is the most important property of melts that controls the dynamic behavior of magmas. Segregation of partial melts in upper mantle and lower crustal sources, magma ascent to shallower depths, intrusion, extrusion as lavas or as explosive fragments, and crystallization all depend on the viscosity of the melt.

Viscosity is formally defined in Figure 6.1a. A force exerted parallel to the surface area of a viscous body produces a shear stress, τ (stress = force/area), that deforms the body by viscous flow in a time-dependent way. This flow deformation can be measured by a velocity gradient, dv/dy, or alternatively by a rate of change in shape, or strain rate, $d\varepsilon/dt$. The proportionality constant relating the shear stress (the "driving force") and the resultant flow is the coefficient of Newtonian viscosity, η

$$6.1 \quad \tau = \eta\frac{dv}{dy} = \eta\frac{d\varepsilon}{dt}$$

For brevity, the coefficient of viscosity can simply be called the *viscosity.*

A convenient way to measure viscosity is by determining how fast a sphere of contrasting density falls or rises through the material (see Stokes law in Section 8.3.3).

The unit of viscosity is the Pa s (Pascal × second) or the poise (10 poise = Pa s). Typical viscosities (in Pa s) include air 10^{-5}; water 10^{-3}; honey 10^{1}; cool asphalt (tar) 10^{8}. Silicate glasses have viscosities $> 10^{12}$. In terms of its atomic structure, glass is a liquid, but in terms of its behavior (atomic mobility and capacity to flow), it is a solid. One way to distinguish between a solid and a liquid is by the time scale for flow. Liquids, such as water and honey, can flow appreciably in minutes because of low viscosity, whereas solids "flow" negligibly, or not at all, over periods measured in years. For example, the solid mantle of the Earth, whose viscosity is on the order of 10^{20} Pa s, convectively flows at a rate of a few centimeters or less per year, the rate of plate motion.

The two principal factors governing viscosity of melts are their composition—as it controls the degree of polymerization—and their T. More polymerized, more silica-rich melts, which have smaller ratios of nonbridging oxygens to network-forming cations (Section 4.1.1), are more viscous. Ions cannot move about readily, especially those that make up polymers, because the strong Si = O and Al = O bonds must be stretched or broken. Less polymerized silica-poor melts and silica-rich melts that contain dissolved water and/or fluorine have lower viscosities. For any melt composition, higher T reduces the viscosity by "loosening" the melt structure through the increased kinetic energy of the atoms; ionic mobility is enhanced.

Figure 6.2 illustrates the strong dependence of melt viscosity on T and composition. For example, the dependence on T is shown by the fact that between 700°C and 1000°C the viscosity of a water-free rhyolite melt decreases by six orders of magnitude, from about 10^{15} to 10^{9} Pa s. The dependence on composition is shown by the fact that there is a difference of about 10^{5} Pa s in viscosities at 1200°C between a silica-poor (46 wt.%) alkali-olivine basalt melt and a silica-rich (77 wt.%) rhyolite melt, both water-free. Besides the silica concentration factor, dissolved water drastically lowers the viscosity of highly polymerized, silica-rich melts because the polymers are broken by hydroxyl ions. Addition of 6 wt.% water to a rhyolite melt with 77 wt.%

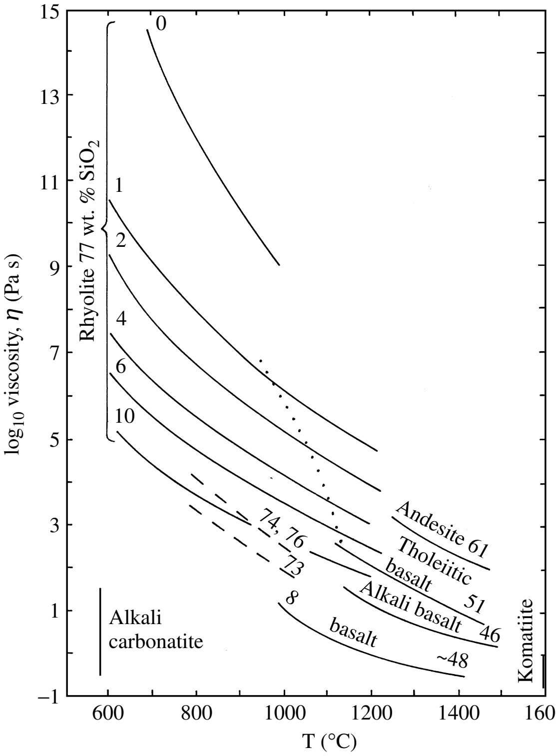

6.2 Newtonian viscosities of some crystal- and bubble-free melts as a function of T at 1 atm. P dependences are negligible. Some viscosities pertain to metastable melts at temperatures below their liquidus where they would contain crystals under equilibrium conditions. Concentrations of silica in weight percentage are indicated as well as of water in weight percentage at low-T end of curves. (Data from Shaw, 1965; Murase and McBirney, 1973; Webb and Dingwell, 1990; Dawson et al., 1990; Huppert and Sparks, 1985.) Viscosities for rhyolite melts that contain 1.5 wt.% fluorine and 6 wt.% water at 10 kbar are dashed lines (peraluminous, 74 wt.% silica; metaluminous, 76; peralkaline, 73). (Data from Baker and Vaillancourt, 1995.) The dotted line indicates the viscosity of residual melts resulting from fractional crystallization of Makaopuhi basalt melt (Table 5.1) with 0.5 wt.% water on the QFM buffer calculated from the MELTS program; the most evolved melt has 73 wt.% silica and 0.3 wt.% water.

silica at 800°C lowers the viscosity by seven orders of magnitude, from about 10^{12} to 10^{5} Pa s. Most of the reduction in viscosity in hydrous silicic melts occurs in the first 2 wt.% or so of added dissolved water because that first 2% is mostly $(OH)^{-}$ (Section 4.2.2). Dissolved water has less effect on basalt melts because they are less polymerized regardless of volatile content. Dissolved fluorine also reduces polymerization and viscosity, but, unlike water, which has very limited solubility in melts at low *P,* fluorine can remain in solution in the melt and can therefore enhance the mobility of lavas extruded onto the surface of the Earth. Rhyolite melts having the lowest viscosity are those that contain both dissolved water and fluorine. The lowest viscosities of any known terrestrial melts are found in ultramafic high-*T* komatiites and essentially silica-free, alkali carbonatites extruded at about 585°C from Oldoinyo Lengai volcano in the East African Rift (Dawson et al., 1990). The 15 orders of magnitude difference in viscosity between carbonatite and dry rhyolite melts extruded near 600°C is illustrated by the contrasting morphological characteristics of their extruded lavas—the former having the appearance of muddy water and the latter forming steep bulbous domes that can be higher than their horizontal diameter. Widespread basaltic lavas that are no more than a couple of orders of magnitude more viscous than cooler carbonatitie melts form sheetlike flows, again in striking contrast with mushroom-shaped rhyolite extrusions.

Melt viscosity is only weakly dependent on *P.* An isothermal increase in *P* of 20 kbar reduces the viscosity of mafic melts by less than 50% and silicic melts by a slightly greater factor (Richet and Bottinga, 1995). This negative dependence on *P* follows because bridging oxygens have a greater molar volume than nonbridging, and, therefore, from Le Chatelier's principle, a positive increment in *P* increases the ratio of nonbridging to bridging oxygens that depolymerizes the melt, reducing the viscosity.

The viscosity of melts that carry suspended crystals (i.e., magma) and contain bubbles of volatile fluid, as well as those that have an intrinsic yield strength do not follow the form of Equation 6.1 (see Section 8.2.2 for a discussion of non-Newtonian magmas).

If a melt is deformed slowly, its distorted atomic structure has time to adjust or relax; it behaves as a liquid. However, for increasingly rapid deformation (increasing strain rate) at constant *T,* particularly in cooler more viscous polymerized melts, the melt crosses a threshold between liquid and solid behavior, called the *glass transition,* defined as the *T* at which $\eta = 10^{12}$ Pa s. If rapid deformation takes place at viscosities above this glass transition, the melt cannot adjust: its **relaxation "time"** is exceeded. It behaves as if it were a solid, breaking as any brittle solid does if the applied stress is excessive.

Advanced Topic Box 6.1 Calculation of melt viscosity

Shaw (1972) developed a model from which the viscosity of homogeneous melts can be calculated from their chemical composition. This model assumes the viscosity follows an Arrhenius relation $\eta = A \exp(-E_a/RT)$ where *A* is a constant, E_a is the activation energy of viscous flow, *R* is the gas constant, and *T* is in degrees Kelvin. Although many melts depart to varying degrees from Arrhenian behavior, Shaw's model has nonetheless proved useful. The full details cannot be dealt with here; only a "cookbook" presentation is given. The viscosity, η, is found from the equation

$$2.303 \log_{10}\eta = s(10^4/T) - 1.5s - 6.4$$

For example, calculation of the viscosity of a hydrous rhyolite (granite) melt at $T = 1073$K ($=800$°C) is presented in Table 6.1, where determination of the value of *s* is described (minor constituents, such as MnO and P_2O_5, are ignored). Numbers in the Moles column are found by dividing the Wt.% values by the Formula wt. of the corresponding oxide. Note that the moles of Al_2O_3 and Fe_2O_3 are doubled. The mole fraction, X, is found by dividing the Moles value by the sum of Moles, or 1.908. In the next column, X_i, the mole fractions of Fe_2O_3, FeO, and MgO are added together (giving 0.009), as are CaO and TiO_2 (0.004), and Na_2O and K_2O (0.057). Shaw's values of the partial molar activation energies of SiO_2 in binary systems with categories of other oxides, s_i^o, are listed in the next column. These values multiplied by the mole fraction of SiO_2 in the particular melt are listed in the $s_i^o X_{SiO_2}$ column. Finally, at the bottom of Table 6.1, the sum of the $X_i(s_i^o X_{SiO_2})$ values listed in the last column is divided by $(1 - X_{SiO_2})$ to give *s,* which is inserted into the viscosity equation. The viscosity calculated from this equation is $10^{5.24}$ poise $= 10^{4.24}$ Pa s. The viscosity measured by Shaw (reference in his 1972 paper) is $10^{4.63}$ Pa s.

Hess and Dingwell (1996) and Baker (1996) have devised models based on experimental data that account for the non-Arrhenian *T* dependence of viscosity for hydrous rhyolite (granite) melts.

In the Shaw, Hess-Dingwell, and Baker models no dependence on *P* is included, as this is negligible.

Ryan and Blevins (1987) have compiled experimentally determined viscosities of a wide range of melt compositions.

Table 6.1 Calculation of the viscosity of a hydrous rhyolite melt at 1073K as described in Advanced Topic Box 6.1.

	Wt.%	Formula Wt.	Moles	X	X_i	s_i°	$s_i^\circ X_{SiO_2}$	$X_i(s_i^\circ X_{SiO_2})$
SiO_2	71.90	60.085	1.195	0.627				
Al_2O_3	12.15	101.961	0.238	0.125	0.125	6.7	4.201	0.525
Fe_2O_3	0.57	159.692	0.007	0.004	0.009	3.4	2.132	0.019
FeO	0.52	71.846	0.007	0.004				
MgO	0.04	40.311	0.001	0.001				
CaO	0.27	56.079	0.005	0.003	0.004	4.5	2.82	0.011
TiO_2	0.09	79.899	0.001	0.001				
Na_2O	3.94	61.999	0.064	0.033	0.057	2.8	1.756	0.100
K_2O	4.32	94.203	0.046	0.024				
H_2O	6.20	18.015	0.344	0.180	0.180	2.0	1.254	0.226
SUM	100.00		1.908					0.881

$s = [\Sigma X_i (S_i^\circ X_{SiO_2})] \div (1 - X_{SiO_2}) = 0.881 \div 0.373 = 2.362$. $2.303 \log_{10} \eta = s(10^4/T) - 1.5s - 6.4 = 2.362(10^4/1073) - (1.5 \times 2.362) - 6.4 = 12.07$. $\eta = 10^{5.24}$ poise $= 10^{4.24}$ Pa s.

Data from Shaw (1972).

6.2 CHEMICAL DIFFUSION

Diffusion, the second transport phenomenon (Figure 6.1b), is the movement of individual atoms or molecules through a group of atoms and driven by a concentration gradient. The material in which atoms are moving does not itself necessarily move. Atoms and molecules diffuse quickly through gaseous bodies where the atoms are widely separated and loosely associated; for example, aromatic molecules from brewing coffee disperse many meters in minutes into the surrounding air. Diffusion is much slower in a liquid and depends strongly on its viscosity and *T;* higher *T* expands the atomic structure and, together with lower viscosity, allows greater freedom of movement for diffusing atoms. Diffusion is still slower in solids where atoms are tightly bonded and have limited kinetic motion relative to those in liquids.

Bowen (1921) first drew attention to the significance of diffusion in magma systems. But it was not until a half-century later, beginning with Shaw (1974), that other experimental petrologists began to explore this important transport process.

Diffusion plays many roles in petrologic processes, some of which are growth of crystals from melts and other multicomponent solutions, exsolution of volatiles from a melt, reaction relations between melt and crystals to produce equilibrium compositions among major as well as trace elements, mixing and contamination of magmas, and isotopic exchange between crystals and fluids. Because the distance over which diffusion takes place depends on time and *T,* measurement of small-scale compositional inhomogeneities within rock-forming minerals and glasses, such as by an electron microprobe, can provide important constraints on their thermal history if the relevant diffusional properties are known. The **closure temperature** at which *T*-dependent diffusion effectively ceases, or becomes nil in a geologic time frame, must be taken into account in interpreting isotopic ages, mineral geothermometers and geobarometers, and any other aspect of a "frozen-in" state of compositional equilibrium.

If rates of diffusion (and other kinetic processes) were infinitely fast, thermodynamic equilibrium would be accomplished instantaneously as changes in intensive variables occurred. However, diffusion is slow in melts and can be extremely slow in crystals, so that vestiges or relics of prior states may be preserved in magmatic rocks. Fortunately for the petrologist, sluggish rates of diffusion can provide insights into prior metastable states and make possible inferences about petrologic history.

6.2.1 Types of Diffusion

Three routes of diffusion are possible in an aggregate of mineral grains, a rock.

1. **Surface diffusion** occurs essentially over a two-dimensional surface area, but generally has a component of atomic movement in the third dimension. Thus, ions can move about over the free surface of a mineral grain through a static liquid in contact with it.
2. **Grain-boundary (intergranular) diffusion** occurs along mutual boundaries between contacting mineral grains. Because of the hindering effects of the adjacent grain, diffusion is slower than for surface diffusion, though both utilize the exterior of a grain. A very thin film of fluid along grain boundaries may facilitate diffusion.
3. **Volume diffusion** occurs within any single homogeneous phase, such as a crystal or a melt body. Volume diffusion through solids is generally the slow-

est, commonly by many orders of magnitude, of the three types of diffusion.

6.2.2 Theory and Measurement

In liquids, atoms have considerable mobility and one atom can collide billions of times a second with its neighbors. In solids, atoms vibrate thermally in a more or less fixed position but can, from time to time, randomly jump by pure chance to a new site. If the concentration of a particular atom varies in some direction, then the random jumps of those atoms will result in a net movement, a flow, or flux, toward the lower concentration region, down the concentration gradient, smoothing out the overall gradient over time (Figure 6.3a).

The mathematical expression, known as **Fick's first law of diffusion,** for the diffusive flow, J_i, of atoms i down their concentration gradient, dc/dx, in the x direction is

$$6.2 \quad J_i = -D_i\left(\frac{dc}{dx}\right)$$

The minus sign that precedes the right-hand expression accommodates the fact that atoms flow spontaneously toward a lower concentration: That is, dc_i is intrinsically negative (Figure 6.1b). The **diffusion coefficient,** or **diffusivity** D_i, has units of square meters per second (m^2/s) and a magnitude related to the frequency at which atoms jump and their jumping distance. Large or highly charged ions strongly bonded with their neighbors jumping through a highly viscous fluid or a crystalline solid have small diffusivities. The transfer rate, or diffusion flux, J_i, can be considered as a ratio of the driving force, dc_i, to the resistance, dx/D_i, for motion of the diffusing atom. In isotropic phases, such as melts, where properties are the same in all directions, the diffusion rate is independent of direction

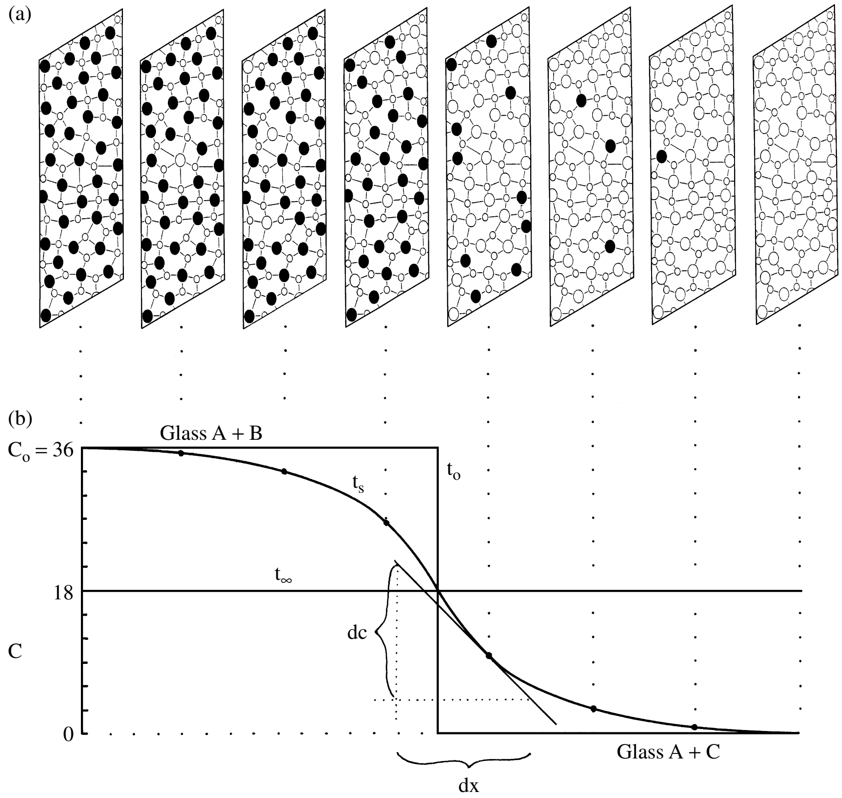

6.3 Schematic atomic diffusion in two contacting hypothetical glasses or melts. Glass on the left that is *initially* composed only of atoms A (small white balls) and B (large black balls) is placed in contact at time t_0 with a glass on the right *initially* composed only of atoms A and C (large white balls). Each glass is assumed to extend infinitely far from their mutual contact: Each is a semi-infinite medium. Because of the initial steplike concentration profile of B atoms, line labeled t_0 in (b), and of C atoms across the contact, B atoms diffuse into the B-free glass on the right and C atoms diffuse in coupled manner into the C-free glass on the left. After some time, t_s diffusion has smoothed the concentration gradient of B atoms, curve labeled t_s in (b), represented in the panel-like slices through the two glasses shown in (a). Note that the glass represented in the three panels on either side of the contact have experienced a change in concentration of atoms B and C whereas the end panels still have the initial concentration. After infinite time, t_∞, the concentration gradient of B atoms is eliminated, straight horizontal line labeled t_∞ in (b), and the two glasses are of the same uniform composition: Concentrations of atoms A, B, and C are the same throughout. In (b), the initial concentration of B atoms in the left glass is c_0 and the scale along the vertical concentration axis is c. The concentration gradient at any position x along the horizontal axis is dc/dx. The equation for the line labeled t_s is the mathematical solution (Jost, 1952, p. 20) for a common experimental setup of Fick's second law of diffusion. Experimentally measurable variables c, x, and t allow evaluation of the diffusivity D.

and only one D value applies. However, most crystals are anisotropic; hence values of the diffusion coefficient and diffusion rates are somewhat different in different crystallographic directions.

Fick's first law describes a steady state in which the concentration profile remains constant through time. But the extent of chemical diffusion in dynamic petrologic systems is time-dependent, expressed in Fick's second law of diffusion, a second-order differential equation (Jost, 1952; Crank, 1975). A graphical solution of this equation is shown in Figure 6.3b for two bodies of glass of contrasting composition juxtaposed along a planar boundary and extending infinitely far in either direction. Another setup might involve a crystal of fayalite (Fe_2SiO_4) in physical contact along a smooth planar interface with a crystal of forsterite (Mg_2SiO_4). At high T, Mg^{2+} ions measurably diffuse into the fayalite and Fe^{2+} ions migrate in the opposite direction into the forsterite. In this case, ionic motion is coupled if electrostatic balance and the appropriate stoichiometrical characteristics of olivine are to be preserved. If left in contact for a sufficient time at high T, the concentrations of Mg and Fe cations become uniform across the two crystals, and they become one homogeneous crystal (if their crystallographic orientations were initially identical).

6.2.3 Factors Governing Diffusivities

The diffusivity, D, of a particular atom in a melt or volatile fluid is inversely correlated with its radius, r, and the viscosity of the medium but directly proportional to T. This relationship is formalized in the **Stokes-Einstein equation**

$$6.3 \quad D = \frac{kT}{6\pi\eta r}$$

where k is the Boltzman constant, T is in degrees Kelvin, and η is the Newtonian viscosity. This model predicts that D is only weakly dependent on P because of the weak dependence of η on P.

The dependence of diffusion on T is described by an Arrhenius equation (equation 3.38 and Worked Problem Box 3.2)

$$6.4 \quad D = D_0 \exp(-E_a/RT)$$

Therefore, the three variables T, D_0, and E_a govern the diffusivity, D, in a solid or liquid medium. The Arrhenius equation indicates diffusion is always more rapid at higher T.

Diffusion in Crystals. In crystals, for relevant magmatic temperatures, the diffusivity, D, ranges over many orders of magnitude. Figure 6.4 shows a range from 10^{-23} m^2/s to 10^{-8} m^2/s. The fastest diffusion is for "trace" diffusion of H_2 along the a axis of Mg-rich olivine and the slowest is for coupled CaAl-NaSi chemical diffusion in bytownite plagioclase, An_{80}. Note the large activation energy for diffusion in plagioclase, 516 kJ/mole, which is not surprising in view of the strong bonding of Al and Si to O. In other words, the slower diffusion of network-forming Si and Al is the limiting rate and not the faster diffusion of network modifying Na and Ca. CaAl-NaSi interdiffusion in plagioclase is more than 10 orders of magnitude slower than diffusion of Na and K in alkali feldspar at about 1000°C, and the difference increases as T decreases. This fact readily accounts for the ubiquity of zoned plagioclases in contrast to the less common, generally more subtle zoning seen in alkali feldspars and other rock-forming minerals. Oxygen isotope exchange in calcic plagioclase is orders of magnitude faster than

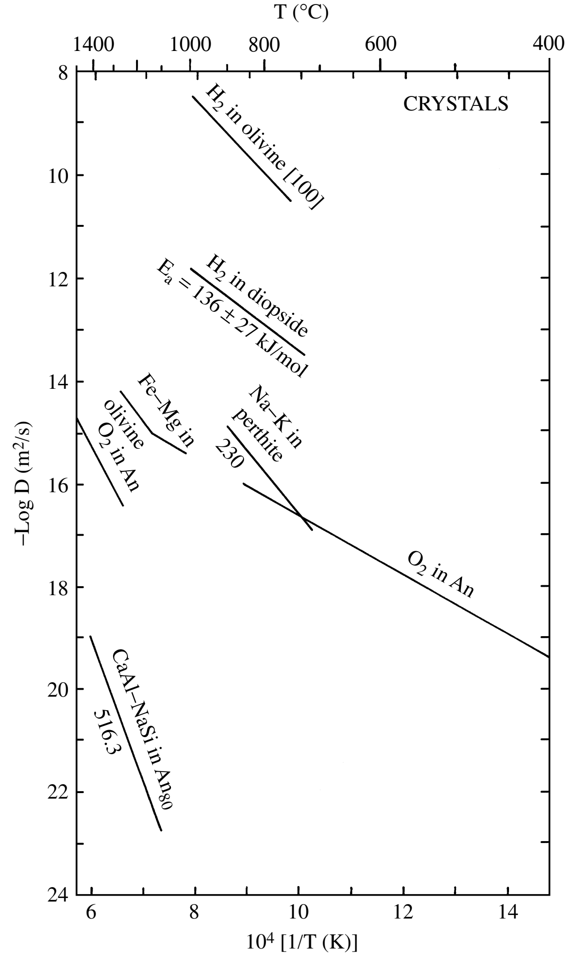

6.4 Diffusivities in crystals. Numbers below lines are activation energies in kilojoules per mole. Diffusion of H_2 in olivine along the a axis [100] and in diopside (in which diffusion appeared to be isotropic). (From Ingrin et al., 1995.) Homogenization of K and Na concentration in a perthite and Fe-Mg coupled diffusion along [001] in olivine. (From Freer, 1981.) Oxygen self-diffusion in anorthite (An) and coupled CaAl-NaSi diffusion in calcic plagioclase An_{80} at 1 atm (homogenizing fine-scale oscillatory zoning). (From Grove et al., 1984.)

CaAl-NaSi homogenization. In the gabbroic Skaergaard intrusion, plagioclases are commonly zoned, yet the oxygen in some of them is from low-T (250–400°C) hydrothermal solutions.

Diffusion in crystals is accomplished by movement of atoms utilizing **point defects** (Figure 6.5). These imperfections in the atomic structure originate as the crystal grows and persist regardless of what subsequently happens to it. Vacancy concentrations are on the order of several per million lattice sites and attain some particular equilibrium value depending upon T.

Diffusion in Melts. Diffusivities are generally larger in melts than in crystals because of the more expanded, or "looser," atomic structure of melts. Figures 6.6 and 6.7 indicate diffusivities that range from 10^{-18} m^2/s to 10^{-6} m^2/s. Comparison of diffusion of univalent alkali metal and divalent alkaline earth ions in water-free rhyolite melt shows that smaller, less charged ions diffuse relatively faster.

Dissolved water reduces the degree of polymerization and the viscosity of rhyolite melts, consequently hastening rates of diffusion of many chemical species by as much as four orders of magnitude (Figure 6.7a). The diffusion of H_2 in hydrous silicic and perhaps basaltic melts is the fastest of any species known thus far. Diffusion of volatiles such as Cl, S, H_2, and CO_2 is enhanced in hydrous melts (Figure 6.7b). Infrared spectroscopy suggests that water diffuses as the H_2O molecule, whereas $(OH)^-$ is effectively immobile. Once H_2O molecules infiltrate dryer melts, they react with bridging oxygens, as in reaction 4.3 (Figure 4.8), to form bridging $(OH)^-$.

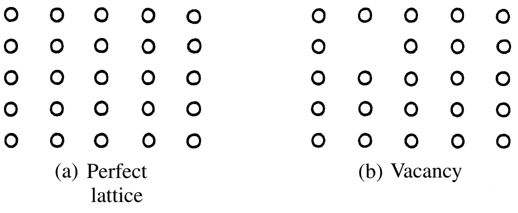
(a) Perfect lattice

(b) Vacancy

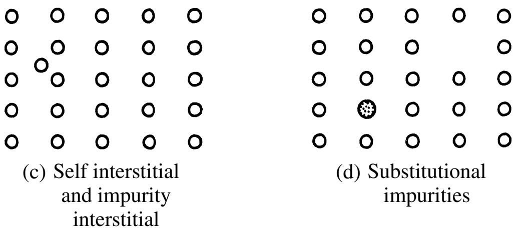
(c) Self interstitial and impurity interstitial

(d) Substitutional impurities

6.5 Schematic types of **point defects** in a crystal lattice. (a) Perfect lattice that never exists in real crystals. (b) Vacancy or Schottky defect is an atom missing from a normal site; an adjacent atom can move into the vacancy and another into its place and so on to accomplish diffusion. (c) and (d) Interstitial, impurity, and substitutional atoms can move through a lattice.

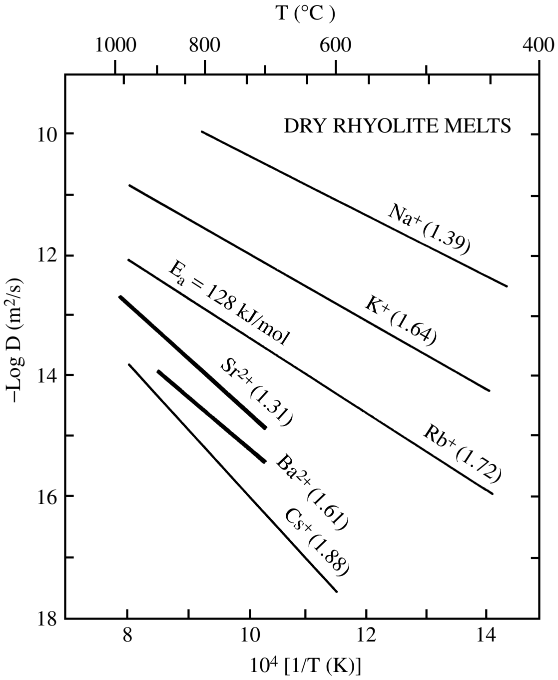

6.6 Diffusivity of some ions in anhydrous rhyolite melt. Numbers in parentheses are ionic radii in ångstroms. (Redrawn from Hofmann, 1980.)

6.2.4 Average Diffusion Distance

A useful relationship first formulated by Einstein in his classic investigation of Brownian movement is

$$6.5 \quad x = \sqrt{Dt} \quad \text{or} \quad t = \frac{x^2}{D}$$

where the diffusion time, t, increases as the square of the "average diffusion distance," or "penetration length," x, and inversely as the diffusivity, D, of the diffusing species. Thus, the time required to double the distance of diffusion for a given D is four times longer. A gas molecule in air at normal atmospheric conditions travels an average distance of 0.1 m in 1 second because $D \sim 10^{-2}$ m^2/s. For silicate melts, a typical $D \sim 10^{-12}$ m^2/s means that an average diffusion distance of about 6 m requires 1 million years (= 3.15×10^{13} s). In a crystal, a diffusivity of, say, 10^{-20}m^2/s allows diffusion over an average distance of only 1 mm (10^{-3} m) in 3.2 million years.

6.2.5 Soret Diffusion

Strictly speaking, diffusion of a chemical species i is driven by a gradient in its chemical potential, $d\mu_i/dx$. For a phase to be in equilibrium, the chemical potential of all components must be uniform; all compositional gradients are smoothed out by diffusion. The chemical potential of i in a phase depends not only on its concentration but also on P and T (Section 3.4.3). Accord-

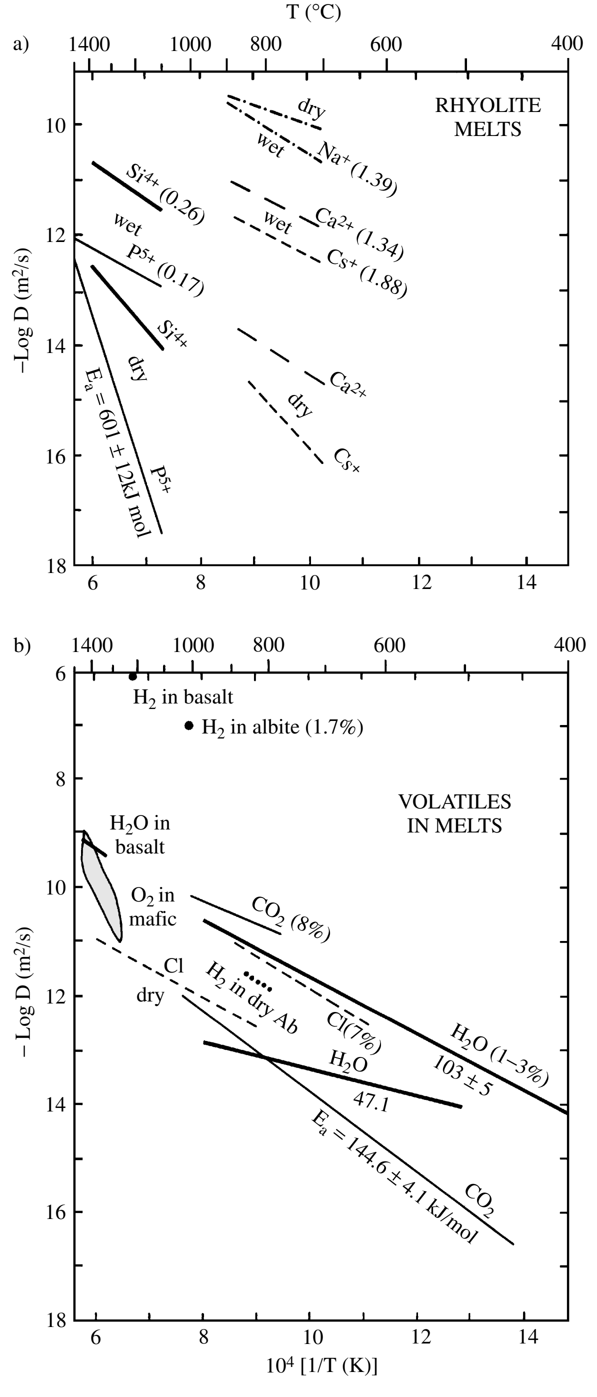

6.7 Diffusivities of some ions in rhyolite and other melts. (a) Diffusion in rhyolite melts that contain 6 wt.% water ("wet") and about 0.1 wt.% ("dry"). Numbers in parentheses are ionic radii in ångstroms. Rare earth elements have similar diffusivities to Si and P. (Redrawn from Watson, 1994.) (b) Diffusion of volatiles in rhyolite melts except as otherwise noted. Bottom three lines are for melts that contain 0.1 wt.% water ("dry"); upper three lines are for melts that contain the (indicated) amount of dissolved water. Shaded lens represents chemical diffusion of O_2 in mafic melts. (Redrawn from Wendlandt, 1991.)

ingly, ions can diffuse in a chemically homogeneous melt that has a thermal gradient. Discovered by C. Soret in 1879, this **Soret diffusion** has been the subject of considerable debate among petrologists concerning its significance in creating diverse compositions from a uniform parent magma (magmatic differentiation). Experiments reveal that relatively smaller network modifying ions of lesser charge, such as Fe^{+2}, Mg^{+2}, and Ca^{+2}, migrate through a thermally nonuniform body of melt from the hotter to the cooler part. Network-forming Si^{+4} and larger network modifying ions, including K^+ and Na^+, remain in the hotter part. However, as chemical gradients so imposed tend to be readily erased by ordinary chemical diffusion and thermal gradients are smoothed even faster (see next section), Soret diffusion is believed to be of little consequence in magmatic systems (Lesher and Walker, 1991).

6.3 DIFFUSION OF HEAT

Heat conduction is the third transport phenomenon of relevance to petrology (Figure 6.1c). As conduction of heat requires transfer of kinetic energy through atomic networks (Figure 6.8), governing equations are similar to those of chemical diffusion. Consequently, heat conduction is often referred to as **thermal diffusion.**

For the variation in T in one dimension, z, Fourier's law for the time rate of heat transfer (compare equation 1.5) is

$$6.6 \quad dq/dt = -k\left(\frac{dT}{dz}\right)$$

where dq is the increment of heat transferred in time dt and k is the **thermal conductivity,** which for rocks is about 2–3 W/m degree. The negative sign is a reminder that heat flows toward the lower temperature. This equation is analogous to Fick's first law for chemical diffusion (Equation 6.2). Another expression for the intrinsic thermal property of a material is its **thermal diffusivity,** $\kappa = k/\rho C$, where C is the specific heat, and ρ is the density. κ is the ratio of the ability of a material to conduct heat relative to its accumulative capacity.

Because it has units of square meters per second, the thermal diffusivity can be compared with the chemical diffusivity, D. The thermal diffusivity is about 5×10^{-7} m^2/s for common dry rocks, but is somewhat less for rocks that contain water or air in pore spaces. Rocks having strongly anisotropic fabric, such as schists, have a slightly greater diffusivity parallel to the foliation than across it. Thermal diffusivities of melts are on the order of 10^{-6} to 10^{-7} m^2/s—as much as eleven orders of magnitude greater than chemical diffusivities (Figures 6.6 and 6.7)! Therefore, static melts solidify by conductive heat transfer well before significant diffusional transfer of ions can occur. Thermal gradients are conductively smoothed much faster than most chemical gradients. However, it will be shown later that more rapid transfer of chemical constituents

(a) Initial time, t_o

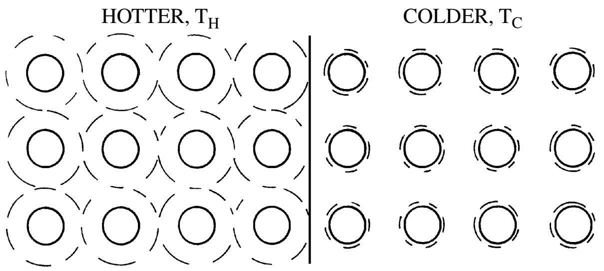

(b) Intermediate time, t_s

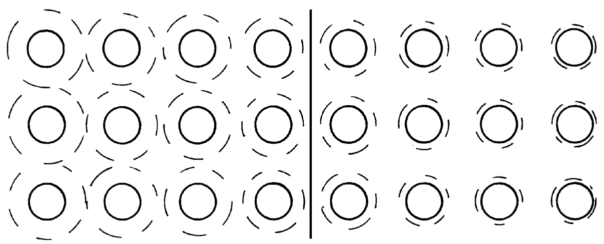

(c) Temperature – time – distance profiles

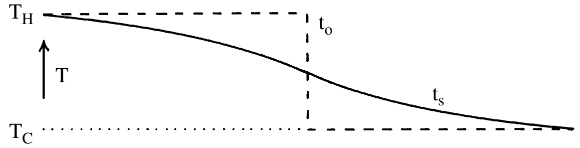

6.8 Schematic atomic model of thermal diffusion or heat conduction. (a) Semi-infinite hotter and colder bodies initially at T_H and T_C, respectively, are brought into contact at time, t_0. Lighter line arcs represent vibrational thermal motion of atoms represented by heavier line circles. Note greater thermal energy in hotter body on left than in colder on right at t_0. (b) After some time, t_s, vibrational energy has been imparted from hotter to colder body in an exponentially decreasing amount from left to right. (c) Graphs of T in bodies at times t_0 and t_s. Eventually, after infinite time, both bodies will be at some uniform intermediate T. Note similarity of smoothed thermal gradient at time t_s to smoothed concentration gradient produced by atomic diffusion in Figure 6.3. In thermal diffusion, however, the kinetic energy of atomic vibration is transferred, whereas in chemical diffusion the atom itself is transferred, a more difficult and slower process.

can take place if the melt is convecting or if fluid bubbles are buoyantly migrating through the melt.

Like chemical diffusion (equation 6.5), a thermal transfer time, *t,* can be defined as

$$6.7 \quad t = \frac{z^2}{\kappa}$$

Thus, *t* increases as the square of the dimension, *z,* of the body. For a constant thermal diffusivity and all other parameters remaining the same, doubling the dimension of a body increases its conductive heating or cooling time by a factor of 4.

6.3.1 The Role of Body Shape on Conductive Cooling

The shape of a conductively cooling body also influences its cooling time. The overall rate of conductive heat loss is a trade-off between the surface area of a body—from which heat is dissipated—and its volume—which holds the thermal energy. The surface area/volume ratio, therefore, controls the rate of conductive heat loss and thermal equilibration between a body and its surroundings, smoothing gradients in *T.* The most thermally retentive shape is a sphere, for which the ratio is least. However, smaller spheres cool faster than larger because their surface area/volume ratio is larger (see Problem 6.6); this is one reason why the small Moon is cold and the Earth is still hot and geologically active. The least thermally retentive shapes are long small-diameter rods and thin sheets because their surface area is large compared to their volume.

Heat is conducted at different rates from different parts of a nonspherical body. For example, in a cube, heat conducts away into the surroundings faster from corners than along planar sides because of the larger mass (volume) of the surroundings into which heat can sink.

❊6.4 INTERFACIAL ENERGY

A brief digression from our discussion of kinetic topics is made here to explore the significant role that the surface area/volume ratio plays in crystal-melt equilibria in magmatic systems. It will be seen that this ratio can have an important bearing on rock texture.

Picture a single cubical unit of halite with the Cl anions and Na cations at alternate corners. Half of the ionic bonds are unsatisfied, so it has a large energy and is, therefore, highly unstable. Within larger atomic arrays, Na and Cl ions have proportionately fewer overall unsatisfied bonds at corners and edges. Thus, larger crystals have a lower surface-related energy and are more stable.

But crystals do not exist in nature as isolated entities; they have some sort of neighboring phases in contact with them. The **interface** between a crystal and its neighboring crystals, melt, or fluid is a layer a few atom diameters thick that differs in structure and thermodynamic properties from the interior of the crystal. The intergrain layer between adjacent crystals is an incoherent mismatch of crystal lattices (Figure 6.9a) where constituent atoms have more energy than interior ones because they are more loosely bonded or have unbalanced bonds. The arrangement of atoms in an interphase layer between crystal and liquid is again different from the crystal interior and has aspects of both phases (Figure 6.9b).

The energy associated with a solid-solid or a solid-liquid interfacial layer is here referred to as the **surface free energy,** γ, with units of joules per square centimeter (J/cm^2) (since the energy is usually related to a particular area). It is defined as the change in energy of the system per unit area of interface generated at constant composition, *T,* and *P.* The creation of a surface re-

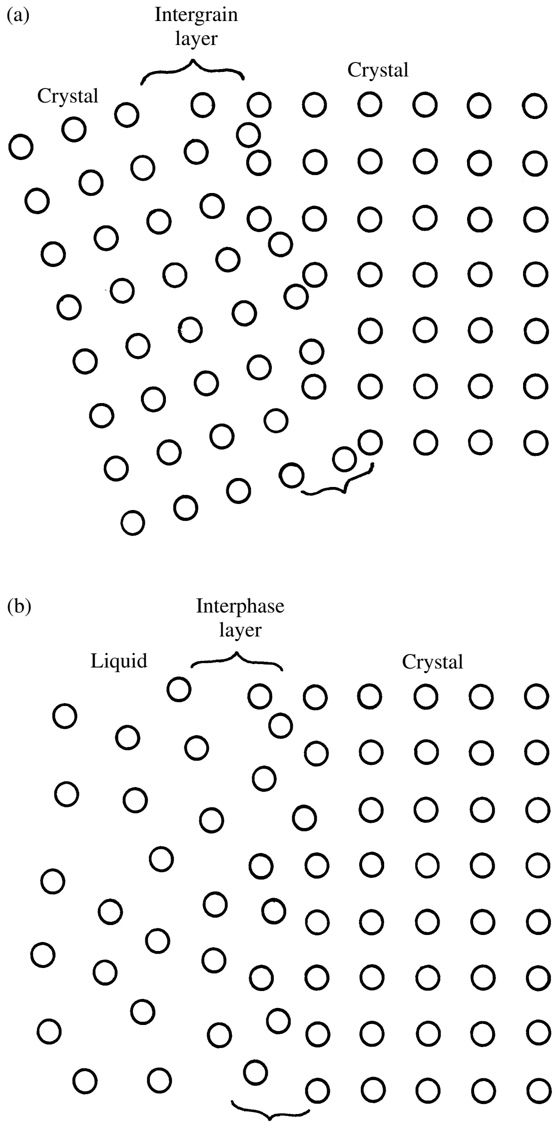

6.9 Schematic diagram of interfacial layers. (a) Intergrain layer between two crystals, either of different phases or of the same phase, showing misorientation of lattices across the interface. (b) Interphase layer between a liquid and a crystal.

quires work, an input of energy, as in cleaving a mineral grain, tearing bonds apart, and creating a free surface.

Because the total energy of a phase is the sum of its surface free energy, γ, and its Gibbs free energy, G, the total energy of progressively smaller volumes of a phase increases as the surface area/volume ratio increases. This means that many small particles are less stable (have greater energy) than one large particle of equivalent volume but lesser surface area (Figure 6.10).

In a liquid body bounded by a gas phase, unbalanced atomic bonds on the surface of the liquid tend to pull it inward, giving rise to a **surface tension.** This attractive force, which has units of energy/area (J/cm^2) like surface energy, makes isolated liquid droplets and soap bubbles spherical, that is, the shape with the smallest surface/volume ratio (lowest energy).

Unlike isolated spherical drops of liquid surrounded by a gas, crystals can possess significantly different surface energies on different crystallographic planes because the geometry of atomic bonding is different; this anisotropy can exist even in isometric crystals. It is the reason why crystals that grow freely in an unrestricted liquid environment are not spheres but have a characteristic crystal habit, such as tabular, platy, or columnar. These **euhedral** crystals are bounded by their characteristic crystal faces. Under equilibrium conditions, crystals growing without any restriction in liquids do so in such a way as to minimize their total energy. Planes of easiest cleavage in feldspars, micas, and amphiboles have relatively lowest energy, and, in these minerals at least, these same planes are developed during crystal growth, minimizing the overall surface energy of the crystal (Kretz, 1966). Hence, in euhedral platy mica, {001} has low energy and is typically prominent, as is {010} in euhedral tabular plagioclase and {110} in euhedral columnar amphibole.

An irregularly shaped, **anhedral** mineral grain bounded by nonrational faces has greater surface free energy than a euhedral crystal of the same phase and volume and is, therefore, less stable than the euhedral equilibrium shape (Figure 6.10).

Therefore, mineral grain sizes and shapes spontaneously adjust toward a state of lower surface free energy. Minimization of the surface energy results in coarser grain size as the surface area/volume ratio is reduced. Modification of grain shape can occur. The minimization principle is an important factor in the

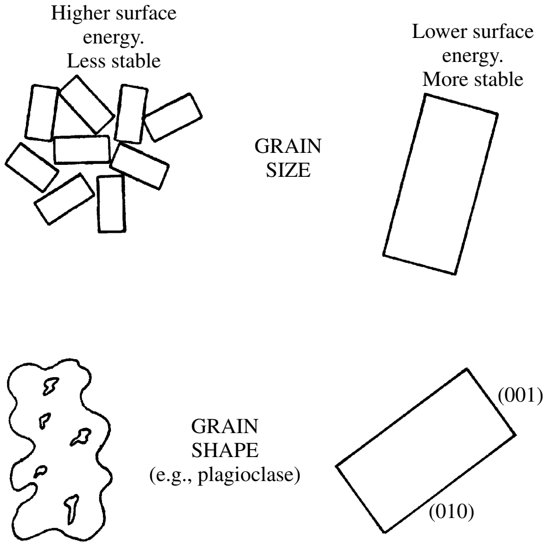

6.10 Influence of grain size and shape on the stability of a phase of *equivalent* volumes (shown schematically here as equivalent areas). One large particle is more stable than many small ones of the same shape because of their greater surface energy contribution. A euhedral crystal bounded by characteristic crystal growth faces is more stable than an irregularly shaped anhedral grain.

evolution of rock fabric, particularly where relatively high rates of diffusion at elevated temperatures are capable of modifying grain boundaries.

Thus, the thermodynamic stability of a phase volume depends on its size and shape, *in addition to P, T,* and concentrations of chemical components (Section 3.4.3).

☼6.5 CRYSTALLIZATION

The three kinetic processes of viscous mobility, transport of atoms, and transport of heat, as well as the tendency of grain systems to minimize their surface free energy, provide a foundation on which to consider crystallization of melts.

Creation of a new phase from any preexisting phase always involves two independent, consecutive kinetic processes—nucleation followed by growth. A growing crystal in a cooling melt must start from an embryonic cluster of ions, called a **nucleus,** probably tens to hundreds of ångstoms in diameter, that possesses all of the characteristics of the crystal. Because the symmetrical lattice of a crystal is usually quite different from the disordered array of ions in a melt, a substantial reorganization of ions is required to produce the crystal nucleus. Once viable, other kinetic factors come into play to allow the accretion of ions onto the nucleus; this is crystal growth. Nucleation phenomena exert a major control on the textures of magmatic rocks, particularly their grain size, as well as their crystallinity and vesicularity. Growth phenomena chiefly influence crystal shapes in magmatic rocks.

Many theories have been proposed for nucleation and crystal growth in melts (summarized by Dowty, 1980; Lofgren, 1980; Cashman, 1990). Most of these models apply to simple, one-component melts so their validity for multicomponent melts in natural magmatic systems is uncertain. In any case, insights from the simple models are useful. As always, the textures of real rocks provide the final test of how correct a theoretical model might be.

6.5.1 Why Is It Important to Study Nucleation and Crystallization?

The application of the material discussed in this chapter to real rocks may seem remote. Connections are mainly deferred to the following chapter on rock fabric. However, to put the discussion of kinetics in perspective it may be beneficial at this point to digress briefly and comment on one of the most fundamental of all rock properties. This property, recognized when a student first becomes acquainted with igneous rocks in the field or laboratory, is grain size.

Igneous rocks obviously possess a wide range of grain size, from submicroscopic (<0.001 mm for an optical microscope) grains to the giant crystals of pegmatites, which can be several meters. This is a range of seven orders of magnitude. Some magmatic rocks have essentially no crystals at all and are instead composed of an amorphous glass. The range in grain size of most rocks is only two to three orders of magnitude. The most common phaneritic plutonic rock—granite—generally has grains 1–20 mm whereas the most widespread aphanitic volcanic rock—basalt—has grains 0.1–1.0 mm. What kinetic process(es) permits such a wide range of grain size but commonly favors a more restricted range? Rate of cooling does control grain size, as usually indicated in elementary geology texts, but is cooling rate the only factor?

If one were to examine thousands of all types of magmatic rocks around the world, it would soon become apparent that some minerals, such as magnetite and olivine, are invariably small, less than a few millimeters, regardless of the magma in which they form. Although phenocrysts of olivine, rarely to as much as 5 mm, occur in basalts, rocks having phenocrysts of magnetite visible to the naked eye (>1 mm) are virtually nonexistent. Upward of 10% Fe-Ti oxides are common in basalts and andesites, for example, but they are invariably small groundmass grains. Even in phaneritic rocks with centimeter-size felsic and mafic silicate minerals, Fe-Ti oxides are generally much smaller. Why is this? What factors allow plagioclases to form phenocrysts 1 cm or more across in many volcanic rocks, and alkali feldspars to form phenocrysts 5 cm across in some granites, and giant crystals meters across in pegmatites? Obviously, cooling rate alone cannot account for the difference in sizes of different crystals growing in the same magma.

Answers to these questions depend on the interplay between nucleation and growth rates for different mineral species in the melt as intensive parameters change in the solidifying magma system.

6.5.2 Nucleation

Countless experiments have amply confirmed W. Ostwald's discovery in 1897 that every phase transformation requires some degree of overstepping beyond equilibrium conditions (Section 3.6.2) to accomplish **nucleation** of a new phase. A second concept is that some phases typically nucleate more readily than others from melts. Kinetic barriers to nucleation are mineral-specific.

Two types of nucleation process can provide a "seed" on which ions in the melt subsequently can accrete during crystal growth: heterogeneous and homogeneous nucleation.

Homogeneous Nucleation. Homogeneous nucleation occurs as a consequence of spontaneous, random fluctuations in the disordered array of ions *within* a uniform body of melt. These transient fluctuations result in a momentary ordered array of clustered ions—a potential nucleus or embryo—that happen to form in the thermally agitating milieu of otherwise disorganized ions. One might imagine a flat tray on which lie closely, but not tightly, packed marbles. If the tray is agitated, momentary clusters of marbles in arrays of sixfold symmetry appear from place to place on the tray and then immediately disappear. Whether similar transient clusters of organized ions in melts can serve as viable nuclei for further accretion of ions during crystal growth depends upon their size and the amount of overstepping—the driving "force" for nucleation.

A new crystalline phase is stabilized once its free energy becomes less than the melt, $G_{crystal} - G_{melt} = \Delta G < 0$. This thermodynamic driving force can be caused by a change in *T, P,* or concentration of some component, or combinations of these changes. Consequently, the melt becomes saturated with respect to the stabilized crystals. Because the most common and easily understood change in geologic systems involves a decrease in *T,* the following discussion focuses on **undercooling** as the means of overstepping.

Very small embryos have a substantial surface free energy, γ, relative to the volumetric $G_{crystal}$ that requires overstepping to become stable (Figure 6.11). At T_e, an embryo of any radius is unstable. For small undercooling, ΔT, small embryos have a relatively large surface energy that makes them unstable with respect to the melt. They might, however, become stable nuclei by growing larger beyond some critical radius, r_c (Figure 6.12). Larger clusters are more stable, but they are less likely to occur by random thermal fluctuations. For large ΔT, even small transient embryos can be stable nuclei because of the increasing difference between the free energies of the crystalline phase and melt, which overrides the surface free energy contribution of the embryo (Figure 6.11). Therefore, the rate of formation of nuclei increases for increasing ΔT. But as T continues to fall below T_e, the probability of transient fluctuations in the atomic array in the melt or parent crystal must decrease because of the decreasing thermal motion of atoms in the increasingly more viscous melt; random fluctuations having the crystalline array are decreasingly likely to occur.

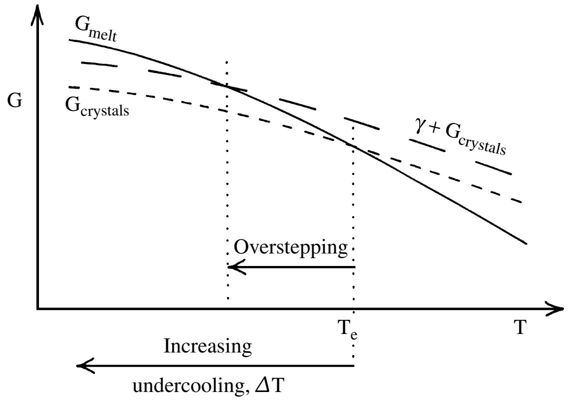

6.11 Schematic plot of free energies of melt and crystal in a one-component system as a function of *T.* Free energies of these two phases are equal and cross over at the equilibrium T_e. The surface free energy, γ, that must be added to the free energy of the crystal phase for very small crystalline nuclei, because of their large surface area/volume ratio, increases their total free energy to the dashed line. Consequently, the cross over of melt and nuclei free energies is shifted to some T below T_e, so that a nucleus can only be stable below some amount of **overstepping** below T_e. The **undercooling,** ΔT, increases to the left below T_e.

Advanced Topic Box 6.2 Theoretical model of homogeneous nucleation

The change in Gibbs free energy accompanying formation of a crystal embryo, assumed to be spherical, from a melt at $T < T_e$ is

$$\Delta G = G_c - G_l = \frac{4/3\pi r^3\ (g_c - g_l)}{V} + 4\pi r^2\ E_s$$

where r is the radius of the embryo, V is the volume of an atom in the embryo, and g_c and g_l are the free energies per atom in the liquid and crystalline states. The $4\pi r^2 E_a$ term is the surface energy contribution of the embryo. For it to be stable, $\Delta G < 0$. The $4/3\pi r^3 (g_c - g_l)/V$ term is negative at $T < T_e$ and ΔG can only become negative when this term exceeds the surface energy term for some increasing r, called the critical embryo radius, r_c (Figure 6.12). For larger ΔT the nucleation driving force, $g_c - g_l$, is an increasingly larger negative number and the $4/3\pi r^3 (gc - g_l)/V$ term exceeds the surface energy term for smaller r_c.

Several complicating factors in the nucleation of multicomponent melts may make this one-component model only a crude approximation to what actually happens. Different minerals in natural melts begin to crystallize at different temperatures and continue to do so over a range of *T.* Increasing cooling in such melts stabilizes solid solutions of changing composition in a melt. Moreover, while one mineral may be nucleating abundantly, another simultaneously stable mineral may not be nucleating or nucleating sluggishly.

Unraveling these sorts of complexities by laboratory studies has proved to be difficult and largely unsuccessful because homogeneous nucleation is a random phenomenon, thus making experimental results inconsistent. The statistically random fluctuations involved in homogeneous nucleation are more likely to occur in less polymerized and therefore less viscous melts; dissolved fluid content, especially water, is thus significant.

Despite the lack of quantitative data, some qualitative inferences have been made regarding relative rates of homogeneous nucleation of common rock-forming minerals. Experimental petrologists (e.g., Kirkpatrick, 1983) have long recognized that minerals with simpler

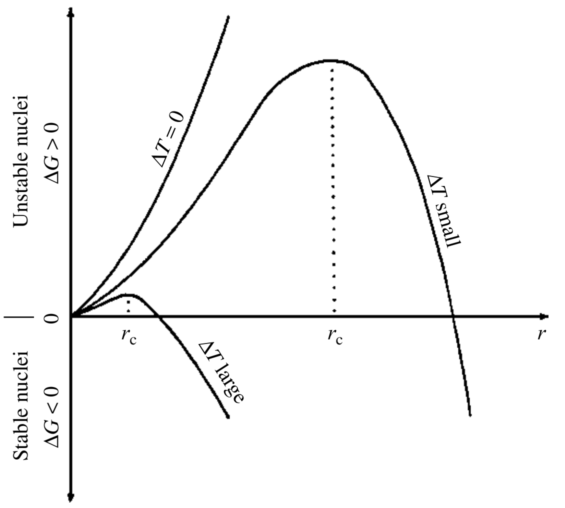

6.12 Relation between radii of homogeneously formed nuclei, r, and free energy in a one-component system at three different amounts of undercooling, ΔT. Nuclei are unstable when $\Delta G > 0$ and stable when $\Delta G < 0$.

atomic structures nucleate with greater ease than tectosilicate (framework) feldspars and quartz in melts of appropriate composition. Carmichael and others (1974, p. 164) have developed a theoretical model in which the nucleation rate is proportional to the square of the entropy change, ΔS_m, during melting of a particular mineral. Small entropy changes occur in melting of cristobalite, albite, and K-feldspar (0.3–0.7 entropy unit per atom in gram formula weight), more for anorthite (1.2), still more for pyroxenes and olivines (1.9–2.1), and greatest for Fe-Ti oxides (2.5–2.6). Minerals with larger entropy change should nucleate more readily, yielding a hierarchy of ease of nucleation, as follows: Fe-Ti oxides (easiest, yielding most abundant nuclei), olivine, pyroxene, plagioclase, and alkali feldspar (least). It may seem surprising that framework silicates would nucleate more slowly from a polymerized granitic melt than mafic minerals and especially Fe-Ti oxides, whose atomic structures are so different. However, greater differences in atomic structure between melt and nucleating mineral, as reflected in the larger entropies of melting, may provide a stronger driving force for nucleation at a particular undercooling.

If these conclusions are valid, they might provide an explanation for the local occurrence of large alkali feldspars and universally small Fe-Ti oxides in magmatic rocks. With only a few nuclei for feldspar-forming components to accrete onto, crystals would be large, and for Fe-Ti oxide components the reverse. (An analogy can be found in growing fruit. To create robust large apples, for example, the orchardist reduces the number of embryonic fruit in some way; in some growing seasons, nature does this by means of a late frost that kills many blossoms.) However, this explanation may be premature because the possible effect of heterogeneous nucleation has not been considered, nor has that of crystal growth rate, which must certainly influence crystal size.

Heterogeneous Nucleation. It is common knowledge that crystals readily nucleate on any existing surface in contact with a melt. This phenomenon is, in fact, a hindrance in experimental investigations of homogeneous nucleation in precious metal containers. The existence of an interface with any contrasting material against the melt can overcome the activation energy barrier so that hetereogeneous nucleation may occur more readily for small ΔT than homogeneous nucleation (Lofgren, 1983; Putnis and McConnell, 1980, p. 104). Existing surfaces can be the solid walls of the melt container or wall rock in the case of a natural magma body.

Existing "seed" crystals in the magma are especially significant in overcoming the difficult nucleation step in crystallization. Overgrowths on the seed are readily facilitated if that phase is stable in the system. Another mineral may also grow around the seed crystal; possible examples are common biotite overgrowths around zircons. Some existing crystals may be earlier-formed crystals. Others may be foreign crystals, or **xenocrysts,** which may have been removed by "erosion" of the wall rock during flow of the magma or introduced into it by mixing with a compositionally contrasting magma. Still other seeds may be **restite crystals** that are undissolved refractory remnants of the source rock from which the magma was generated by partial melting processes in the deep crust or mantle.

Minute crystalline entities, microscopically invisible, may serve as seeds for crystal formation. These might have survived an episode of brief melting above the liquidus and could be of restite or xenocryst derivation in magmas extracted rapidly from their source. Some melts seem to have a "memory" of their thermal history—such as how long they were heated at a particular T above the liquidus—that influences their crystallization behavior below the liquidus.

Other potential interfaces for heterogeneous nucleation are walls of volatile bubbles in the melt (Davis and Ihinger, 1998). In this case, there can be an interplay, even feedback, between exsolution of fluid from the melt and nucleation. Crystals nucleate and grow on bubble walls, causing more saturation of fluid in the melt, which leads to more exsolution, and so on.

Many petrologists believe that heterogeneous nucleation is common, if not dominant, in natural magmas. However, there is little conclusive data to confirm this belief.

6.5.3 Crystal Growth

Once nuclei are viable, growth of crystals can occur as additional ions become attached. Like nucleation, the rate of crystal growth is related to the degree of undercooling of the system, ΔT (Figure 6.13). Increasing

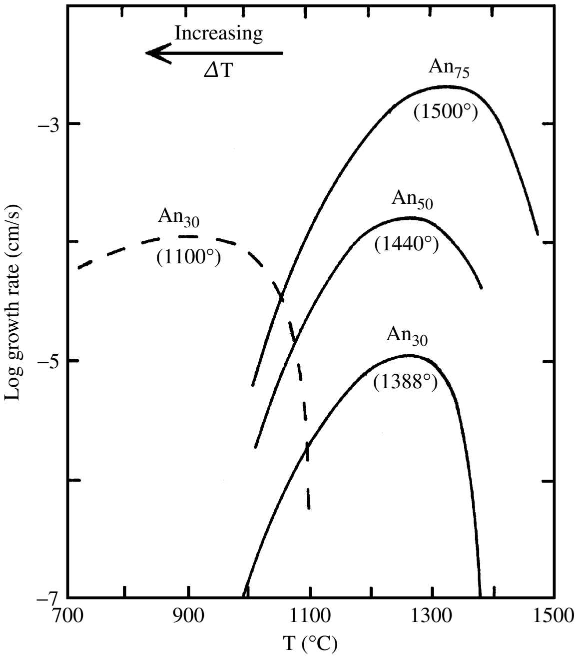

6.13 Experimentally determined plagioclase growth rates as a function of degree of undercooling, Δ*T*, in their equivalent melts. The composition of the crystals is indicated in mole percentage and the corresponding liquidus *T* is in parentheses below each curve. Solid lines are in dry melts at 1 atm; note decreasing peak growth rate at decreasing *T*. Dashed line is for growth in a water-saturated melt at 2 kbar; the dissolved water depolymerizes the melt and promotes faster peak growth, despite the lower *T*. (Redrawn from Lasaga, 1998; see also Fenn, 1977.)

undercooling provides a stronger driving force for growth, but with falling *T* the increasing melt viscosity retards ionic mobility. For this reason, the growth rate is a bell-shaped curve.

There are more experimental data on crystal growth than on nucleation in geologically relevant melts. Some experiments report data in terms of the degree of undercooling, Δ*T*, others in terms of the cooling rate, Δ*T*/Δ*t*. These parameters are obviously related, but in dynamic magma systems the latter is more meaningful than an apparent one-step drop in *T* implied in a Δ*T* value.

Influence of Undercooling on Crystal Shape. Many experiments on crystal growth (e.g., Lofgren, 1980; Swanson and Fenn, 1986) have demonstrated that as Δ*T* and Δ*T*/Δ*t* increase, crystals increasingly depart from an equilibrium habit of characteristic crystal faces. This departure from euhedral shapes occurs because, with changing intensive parameters in the system, usually falling *T*, diffusion of atoms in the cooler, more viscous melt and conduction of latent heat away from the growing crystal are less able to keep up. Crystals become less compact with increasing Δ*T* and Δ*T*/Δ*t*.

Actual grain shapes vary with respect to the particular mineral, melt composition, and amount of undercooling. A general pattern seen in laboratory experiments can be illustrated with plagioclase as an example (Figures 6.14 and 6.15). For Δ*T*/Δ*t* less than a few degrees/hour (Δ*T* less than tens of degrees), crystals have a euhedral tabular habit; these are typical of phaneritic plutonic rocks and slowly grown phenocrysts in volcanic rocks. For Δ*T*/Δ*t* of tens of degrees/hour (Δ*T* on the order of 100°C) crystals are hollow, **skeletal,** and H-shaped forms; these are found in some glassy and aphanitic volcanic rocks. For greater Δ*T* and Δ*T*/Δ*t*, **dendritic,** branching, and **feathery** forms develop. For Δ*T*/Δ*t* of hundreds of degrees/hour and very high effective Δ*T*, radiating, three dimensional sprays of fibrous to needlelike crystals called **spherulites** develop, probably after the melt drops below the glass transition ($\eta > 10^{12}$ Pa s). Rapidly cooled submarine basalt pillow lavas show dendritic and skeletal forms as well as radiating intergrown plagioclase and pyroxene.

These kinetically controlled crystal habits result from different factors during the growth process, including the following:

1. Phenomena at the crystal-melt interface as ions become attached to the surface of the growing crystal
2. Diffusion of ions through the melt to the growing surface
3. Removal of latent heat of crystallization from the crystal-melt interface
4. Viscous flow of melt past the crystal face

Whichever of these kinetic rates is slowest dictates the overall rate of growth. In a one-component system, such as ice crystals growing in water, diffusion and viscous flow are irrelevant because necessary ions in the proportions of the crystal are everywhere and always present, but ion attachment to and dissipation of latent heat from the growing crystal face are rate-controlling. In multicomponent melts, interfacial reactions, diffusion, and dissipation of latent heat appear to be significant, in that order, for increasing Δ*T* and Δ*T*/Δ*t*.

In the growth of robust, compact crystals having characteristic habits (tabular, prismatic, etc.) the controlling process is the attachment of ions to the growing crystal face (Dowty, 1980; Kirkpatrick, 1981); this is interface-controlled growth. Chemical diffusion is relatively rapid near liquidus temperatures and still faster dissipation of heat can keep pace with the slow cooling rate of the melt. However, even for slow growth in the plutonic environment, euhedral plagioclases generally have slight compositional zoning that indicates perfect equilibrium was not attained because, once a crystal forms, adjustment of the CaAl/NaSi ra-

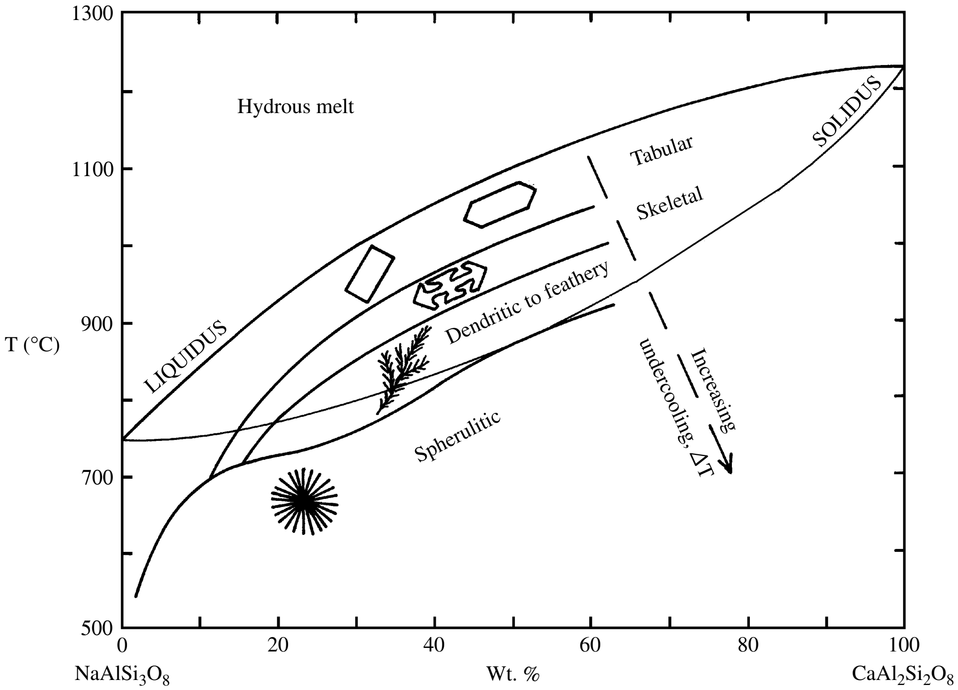

6.14 Schematic shapes of experimentally grown plagioclase crystals in a melt depend on the amount of undercooling, ΔT. Compare Figure 5.13. Heavier lines delineate regions of undercooled-controlled crystal morphology, schematic representations of which are shown. Compare photomicrographs of actual crystals in Figure 6.15. (Redrawn from Lofgren, 1980.)

tio in it by diffusion-controlled reaction relations is exceedingly slow.

Crystal forms become more open and skeletal and have an increasing number of reentrant angles at increasing ΔT and $\Delta T/\Delta t$. Dendritic and feathery crystals have yet larger (disequilibrium) surface area/volume ratios. Growth may result from the need to dissipate latent heat, as exemplified by wintertime formation of feathery ice crystals on windows. The exact way in which exponentially decreasing rates of chemical diffusivity with decreasing T enter into crystal growth is not clear, although many theoretical models have been proposed.

Compositional Boundary Layers and Implications. Compositional gradients defining a **compositional boundary layer** can develop in the melt beside a growing crystal (Figure 6.16). While incompatible ions become enriched in the layer compatible ions become depleted, slowing crystal growth. For growing solid solutions (e.g., plagioclase) the boundary layer becomes depleted in the high-T component ($CaAl_2Si_2O_8$) and enriched in the low-T component ($NaAlSi_3O_8$) relative to the melt outside the layer. In some way, which is not yet completely understood, kinetic phenomena in boundary layers adjacent to growing plagioclases in intermediate composition magmas create fine-scale oscillatory zoning in the crystal (Figure 6.17). In hydrous melts, growing anhydrous crystals create a boundary layer enriched in water that hastens chemical diffusion, depresses the liquidus, and possibly locally saturates the melt in water.

Small volumes of melt, called **melt inclusions,** can be entrapped within a growing crystal (Figure 6.18).

If convective movement of the melt in the boundary layer beside a growing crystal is negligible, then incompatible components can become saturated in the boundary layer and a new phase can be stabilized (Bacon, 1989) including accessory apatite (incompatible P) and zircon (Zr).

6.5.4 Crystal Size in Magmatic Rocks

We return now to the question posed in Section 6.5.1, namely, What controls grain size in magmatic rocks?

The number of nuclei in a volume of melt, called the **nucleation density,** is the integrated effect of a varying rate of nuclei formation over some period. During this time, crystal growth is probably also taking place, consuming the mass of necessary chemical components in the melt for a particular mineral. If the growth rate is relatively slow, many nuclei might form before the mass is consumed; grain size would consequently be small, perhaps aphanitic. This occurs typically in volcanic environments where the rate of cooling of melts is relatively fast, or in some plutonic situations where a sud-

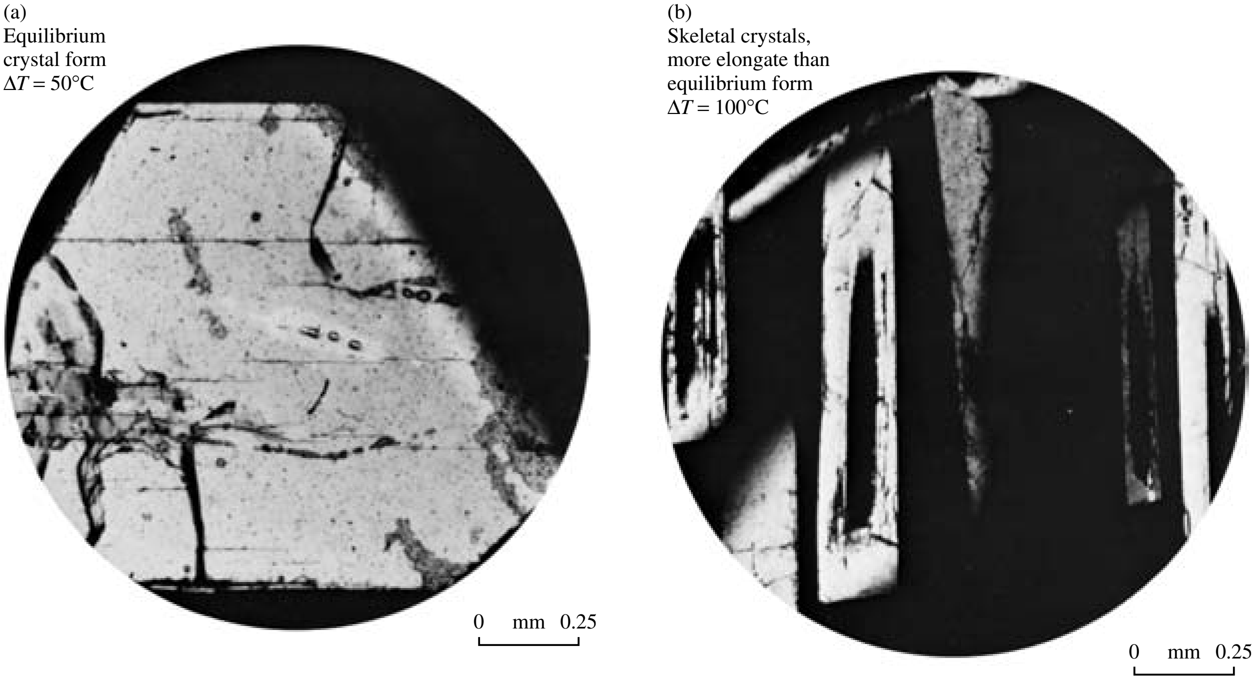

(a)
Equilibrium
crystal form
$\Delta T = 50°C$

(b)
Skeletal crystals,
more elongate than
equilibrium form
$\Delta T = 100°C$

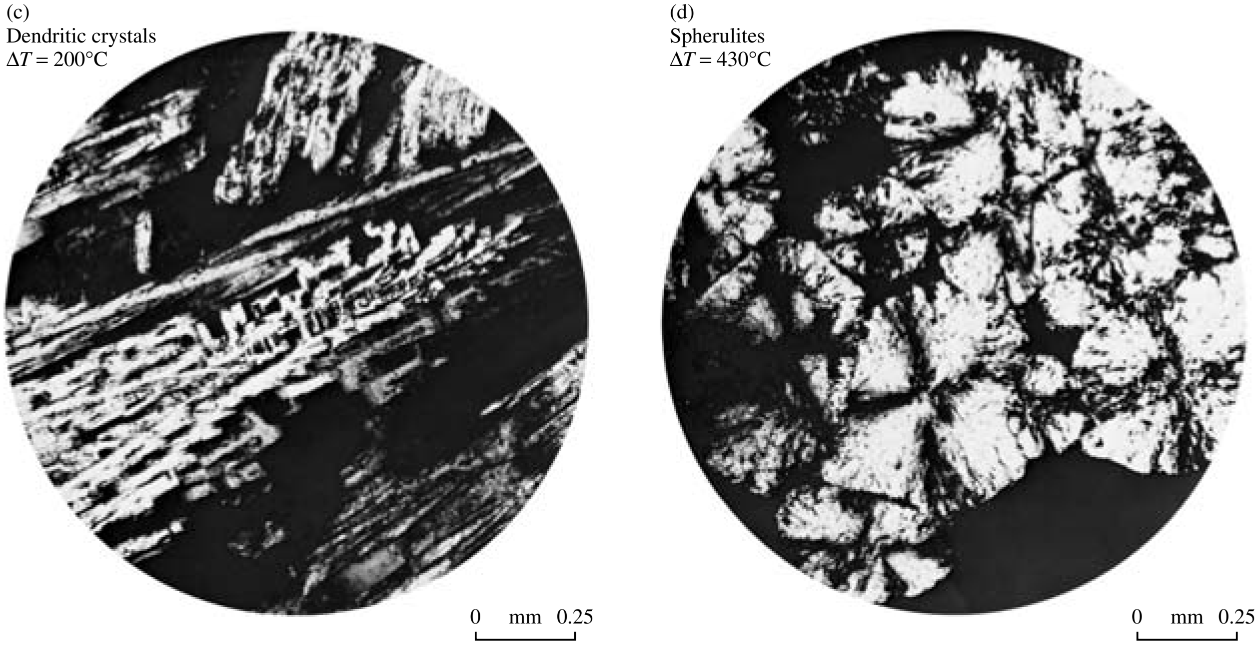

(c)
Dendritic crystals
$\Delta T = 200°C$

(d)
Spherulites
$\Delta T = 430°C$

6.15 Shapes of plagioclase crystals grown experimentally from melts as a function of undercooling, ΔT. Photomicrographs under cross-polarized light. **Spherulites** are radiating spherical aggregates of fine needlelike crystals that are optically extinguished in the N-S and E-W directions, forming the black crosses. (Photographs furnished by Gary E. Lofgren and NASA. Reproduced by permission from Lofgren GE. An experimental study of plagioclase crystal morphology. Am. J. Sci. 1974; 274:243–273.)

den release of water occurs to create a pressure quench, forming a porphyry. Some melts, especially highly viscous ones, can thermally quench to form glass. If, on the other hand, growth rate is fast relative to nucleation rate, then fewer nuclei form by the time the mass is consumed; the grain size is larger, perhaps phaneritic but possibly more variable. This occurs typically in deep confined plutonic settings where heat loss is slow.

Shaw (1965; see also Brandeis and Jaupart, 1987) proposed that grain size is proportional to the ratio of crystal growth rate, $\mathcal{G}$, to nucleation rate, N,

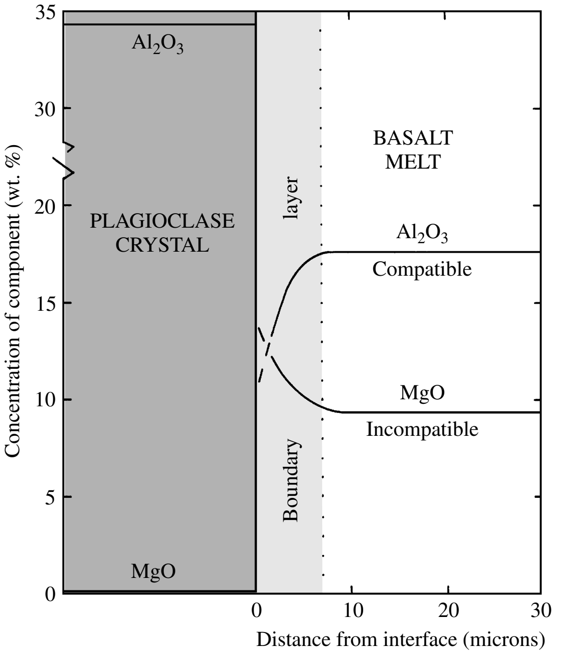

6.16 During relatively rapid growth of a crystal, concentration gradients form in the melt adjacent to the crystal and define a **compositional boundary layer.** Compatible elements, such as Al, diffusing to the growing crystal of plagioclase (about An_{86}) in the basalt melt define an exponentially decreasing concentration in the boundary layer adjacent to the crystal. Incompatible elements, such as Mg, mostly excluded from the growing crystal, must diffuse away from it and form an exponentially increasing concentration toward the crystal. Uniform concentrations of chemical elements on each side of the boundary layer in the basalt melt and plagioclase crystal are indicated by straight horizontal lines. Concentrations of oxides of the elements shown here were determined by electron microprobe analyses. (Modified from Bottinga et al., 1966.)

$$6.8 \quad \text{average crystal size } \alpha\left(\frac{\mathcal{G}}{N}\right)^{1/4}$$

Extrapolation of theoretical and experimental studies of nucleation and crystal growth in simple, usually one-component systems to multicomponent natural melts is a tenuous step and has not led to a thorough understanding of the kinetic factors governing such a fundamental rock property as grain size. Attempts to quantify kinetic factors from textures of real rocks in the simplest of thermal environments—such as a thin basaltic dike—have met with limited success. The fact that some granitoid plutons contain quite variable grain size on an outcrop scale whereas others have strikingly uniform grain size throughout tells us that overall cooling rate and magma composition are not the whole story. What role does the distribution of water or some sort of seeds in magmas play?

Investigations by chemical engineers into industrial crystallization have yielded insights into the kinetics of crystallization. Their concepts have been adapted to rocks by Marsh (1988) and have been applied to basalts and silicic volcanic rocks by Cashman (e.g., 1990).

❊6.6 SECONDARY OVERPRINTING PROCESSES MODIFYING PRIMARY CRYSTAL SIZE AND SHAPE

Two additional factors that play roles in governing magmatic grain size and shape are crystal dissolution and secondary equilibration of grain margins after primary growth.

6.6.1 Crystal Dissolution

Resorbing reaction relations are common in magmas, consuming, to varying degrees, previously precipitated phases (e.g., olivine in Makaopuhi basalt magma, Figure 5.10, and quartz phenocrysts in decompressing rhyolite magma, Section 5.5.5). Dissolution of crystals occurs during mixing of dissimilar crystal-laden magmas that are striving to reach a state of internal equi-

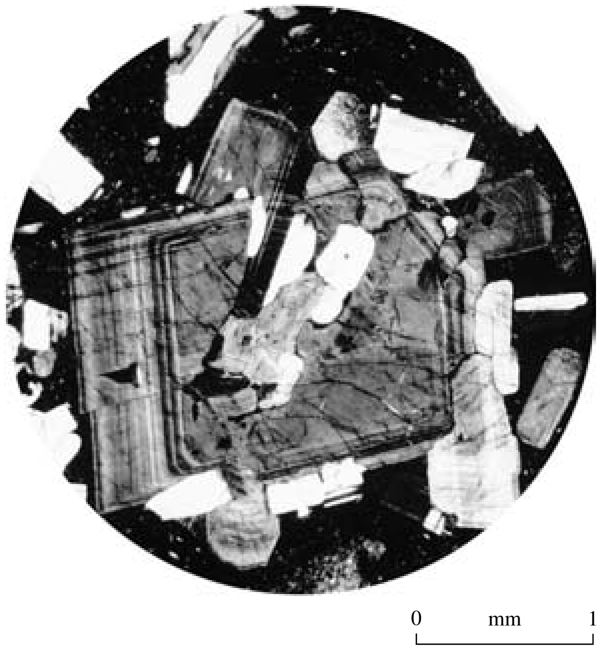

6.17 **Oscillatory zoning** in plagioclase in an intrusive diorite porphyry, central Utah. Photomicrograph in cross-polarized light. Thin concentric zones have differing optical extinction orientations that manifest an alternating relative enrichment in albitic and anorthitic end members from one zone to the next. The zoning is usually not strictly oscillatory, as is a sine function; each peak increases in Ab content away from the crystal center and drops more sharply. Peaks are typically 5–15 mole % in amplitude and the wavelength is 10–100 micrometers. These oscillations are commonly superposed on a larger-scale normal zonation toward a more sodic rim. The cluster of grains defines **cumulophyric** texture. See Pearce and Kolisnik (1990) for further description of oscillatory zoning in plagioclase.

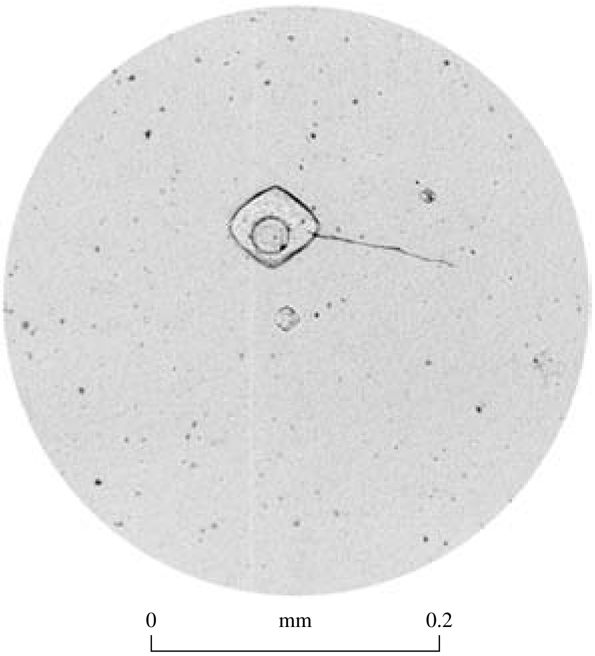

6.18 **Melt inclusions** (now glass) in quartz phenocryst in silicic volcanic rock. Photomicrograph under plane-polarized light. The three inclusions quenched from melt entrapped in host quartz crystal as it was growing. Inclusions have a slightly smoothed rhombohedral "negative crystal" form that indicates the melt and crystal were in equilibrium at entrapment. Spherical fluid bubble in largest inclusion is of uncertain origin; it may not indicate volatile saturation at time of entrapment. Line is a crack in host crystal.

librium and during the evolution of magmas that contain unstable restite crystals and assimilated xenocrysts from foreign country rock.

Partially dissolved crystals of different origins are evident in many volcanic rocks and are preserved because the magma solidified more rapidly than the crystal could completely dissolve; such is generally not the case in more slowly cooled and more nearly equilibrated plutonic systems. Unstable crystals are readily apparent from their embayed and corroded forms and, in volcanic rocks, abundance of irregularly shaped melt inclusions (now glass; Figure 6.19). Some rocks preserve partially resorbed crystals rimmed by a later precipitated phase or assemblage of phases—a reaction rim between the dissolving crystal and the enclosing melt (Figure 6.20). For example, a quartz xenocryst plucked off the wall rock and incorporated into a basalt melt dissolves because the melt is undersaturated in silica (silica activity <1; Section 3.5.3). Dissolution of foreign material is called **assimilation;** it contaminates the magma and contributes to the wide compositional diversity of magmas and igneous rocks on Earth.

Relevant kinetic processes for dissolution might involve reactions at the crystal-melt interface, diffusion, absorption of heat by the crystal, and convective movement of the melt beside the crystal—the same factors involved in crystal growth. Zhang et al. (1989) find that the melt immediately adjacent to a dissolving crystal saturates with its constituents almost instantaneously, so that convective processes are required for continued effective dissolution. The rate of dissolution is proportional to the square root of time. At low *P* and moderate undersaturation, felsic minerals and pyroxenes dissolve faster than olivine, which dissolves faster than accessory minerals. This is a trend of generally decreasing solubility and mirrors the trend of ease of nucleation cited previously. These solubility differences could play an important role in which minerals are most likely to be preserved as restite crystals in magmas ascending out of their source.

6.6.2 Textural Equilibration: Grain Boundary Modification

An underappreciated and little understood phenomenon that also affects magmatic grain size and shape involves secondary reequilibration of grain margins as an aggregate strives to minimize its surface free energy (Section 6.4). Textural equilibration is favored if temperatures remain high in the system. Concepts of textural equilibrium developed chiefly by metallurgists have been applied to magmatic textures by Maaløe (1985) and Hunter (1987), among others.

6.19 **Partially resorbed** quartz phenocryst in silicic volcanic rock. Photomicrograph under plane-polarized light. Deep, irregularly shaped embayments indicate crystal was unstable in the melt prior to its solidification into an aphanitic groundmass. Irregularly shaped apparent inclusions embedded in quartz crystal may only be narrow embayments extending from third dimension.

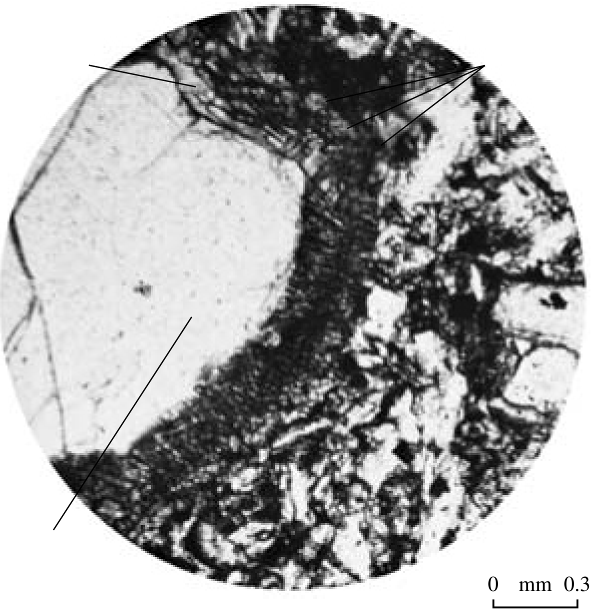

6.20 **Partially resorbed** quartz xenocryst in a basalt surrounded by a reaction rim of minute rod-shaped clinopyroxenes.

Modification of Grain Size. Crystal size can increase by the process of **Ostwald ripening** (Figure 6.21). Large and small crystals of the same phase dispersed in a communicating fluid or melt at fixed P and T are relatively more and less stable, respectively, because of their differences in surface free energy per volume (Figure 6.10). Consequently, smaller crystals tend to be consumed at the expense of larger, more stable grains. (This is the petrologic counterpart of the economic dictum that the rich get richer and the poor get poorer.) The result of this equilibrating "ripening" is an overall increase in average grain size of the system. Jurewicz and Watson (1985) experimentally confirmed that in a partially crystallized granite magma held at constant P and T for several days, average quartz grain diameter increased while number of grains decreased. Grain diameter adjustment was a response to minimization of surface energy, not progressive growth because the overall volume of quartz remained constant. Park and Hanson (1999) observed the same phenomenon for olivine in a model basalt system.

Modification of Grain Shape. In Ostwald ripening, grain shape may be modified as well as grain size, both according to the requirement to minimize surface free energy. Therefore, cooling rates initially control shapes of crystals growing freely in a melt (Figures 6.14 and 6.15), but subsequent modifications in shape may occur, if time and diffusion rates permit.

Consider three grains A, B, and C in mutual contact. A cross section drawn perpendicular to this common grain-boundary line defines a triple point between the grains cited (Figure 6.22). Interfacial energies between the grains, γ_{AB}, γ_{BC}, and γ_{AC} can be considered as surface tensions and represented as force vectors. At equilibrium, these must sum to zero around the triple point. For a particular set of crystalline phases whose interfacial energies are dictated by their compositions, T, and P, equilibrium is achieved by the grains adjusting their mutual angles, α, β, and δ, at the triple point so that

$$\frac{\gamma_{AB}}{(\sin\alpha)} = \frac{\gamma_{BC}}{(\sin\beta)} = \frac{\gamma_{AC}}{(\sin\delta)} \tag{6.9}$$

If all three grains have the same interfacial energy, the three interfacial angles must be equal, or 120°, because they must sum to 360°. A tightly packed, void-free aggregate of polyhedrons that have uniform volume and minimal overall surface area and, therefore, surface energy is shown in Figure 6.23. In such an aggregate viewed in thin section, triple-junction interfacial angles approach 120°. This geometry is seen in very slowly cooled gabbroic and phaneritic ultramafic rocks (Figure 6.24). A remarkably similar geometry is found in highly vesicular glassy basalt (Figure 6.25), where gas-bubble shape is dictated by surface tension. The extent to which the angle is near 120° (but see Kretz [1966] for exceptions) in mineral aggregations means that the grains had similar interfacial energies, regardless of their crystallographic orientation. Interfacial angles were balanced and grain boundaries migrated during prolonged textural adjustment at elevated T by means of differential solution and growth via atomic diffusion.

Different crystallographic surfaces of a crystal actu-

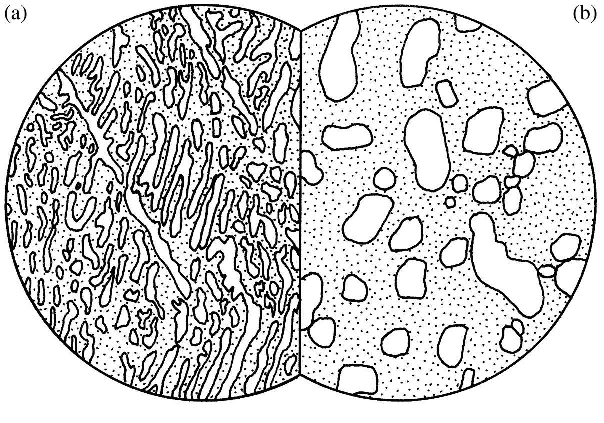

6.21 **Ostwald ripening** of ammonium thiocyanate dendrites. Grain coarsening in this low-T organic compound models what may happen in a high-T silicate system. (a) Immediately after cooling to 50°C the initial single-crystal dendrite has already segmented into discrete rods within the melt (stippled). (b) Same field of view as (a) after 9.8 hours. The initial dendritic crystal with a large surface area has been stabilized by formation of larger crystals with overall lesser surface area; crystal volume remained the same. Note that the isolated crystals in (b) *did not individually nucleate.* Field diameter is about 0.4 mm. (Drawn from a photomicrograph in Means and Park, 1994.)

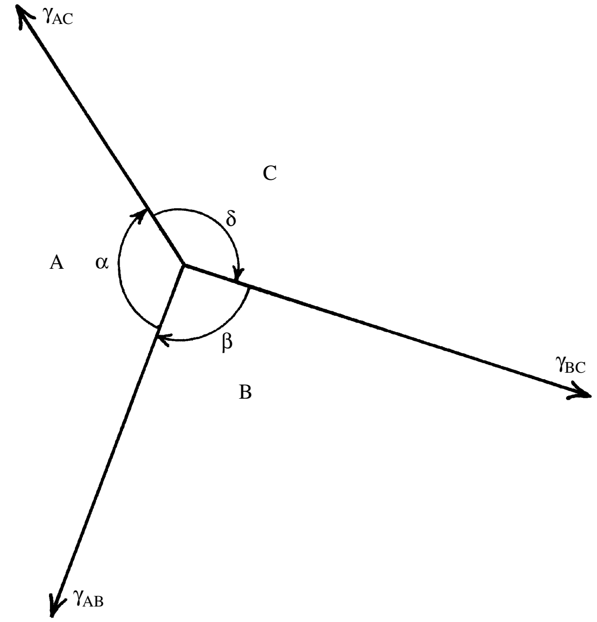

6.22 Intergrain surface free energies. These energies, γ_{AB}, γ_{AC}, γ_{BC}, are represented by vectors along boundaries of grains about a triple-grain boundary junction of three grains A, B, and C.

ally have different energies. The lowest-energy faces stabilize the crystal volume during growth. In plagioclases grown from melts the typical habit is tabular with largest faces parallel to {010}. This suggests preferred growth on higher-energy faces parallel to {100} or {001} so that the lowest-energy and most stable {010} faces dominate the enclosed volume.

An example of how this variable surface energy might influence crystal shapes of contacting grains in a magmatic rock is shown in Figure 6.26. Although the validity of extrapolating grain boundary modification in a low-*T* ammonium compound, as in this figure, to high-*T* silicate systems can be questioned, the obvious textural adjustment of the former should convince us to be cautious in the interpretation of the latter.

6.7 VESICULATION AND FRAGMENTATION OF MAGMA

Exsolution of volatiles from melts that produce fluid bubbles—the process of **vesiculation**—has many parallels to crystallization that produces crystals. Bubbles are preserved in solidified rock as **vesicles.** Both vesiculation and crystallization follow kinetic paths of nucleation and then growth. Both kinetic paths accompany changes in the state of the magma system caused by changes in intensive parameters, chiefly decreasing *T* and *P.* Crystallization during cooling and decompression during ascent induce exsolution of volatile fluids from initially volatile undersaturated melts (Section 4.2.3). The increasing mass of exsolved volatiles, chiefly water in most systems, compounded by volumetric expansion of the volatile fluid at decreasing *P,* causes bubble growth and potential fragmentation of the magma during explosive volcanism. This and other consequences of volatile exsolution are discussed in Section 4.3. Kinetic processes of magma degassing near the surface of the Earth are the focus of this section.

6.7.1 Nucleation and Growth of Bubbles—Vesiculation

Nucleation. According to homogeneous nucleation theory, energy is required to create the interface of an embryonic cluster of volatile molecules that originate by random fluctuations in their concentration in the melt (Sparks et al., 1994). As for crystal nucleation, only clusters of a critical radius are stable with that radius determined by the Gibbs free energy difference between melt and the surface free energy of the cluster (compare Figures 6.11 and 6.12 for nucleation of crystals).

In experiments on bubble nucleation in a hydrous rhyolite magma, Hurwitz and Navon (1994) found no

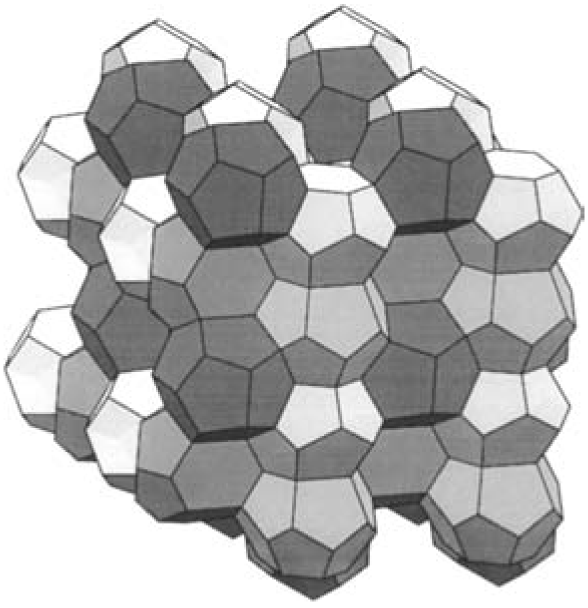

6.23 An array of polyhedrons that has minimal surface area. The equal-volume polyhedrons are of two types: 14-sided polyhedrons of 12 pentagonal and 2 hexagonal faces and 12-sided polyhedrons of 12 faces that are somewhat distorted pentagons (Weaire and Phelan, 1994). This minimal surface area geometry is found in aggregates of soap bubbles and vesicles in thread-lace scoria (Figure 6.25). It is also approximated in some crystalline aggregates (e.g., Figure 6.24) in which there has been textural adjustment over long time at high *T.* In two-dimensional slices, bubble or grain boundaries have $\sim$120° triple junctions: $\alpha = \beta = \delta = 120°$ in Figure 6.22. (Image courtesy of Ken Brakke.)

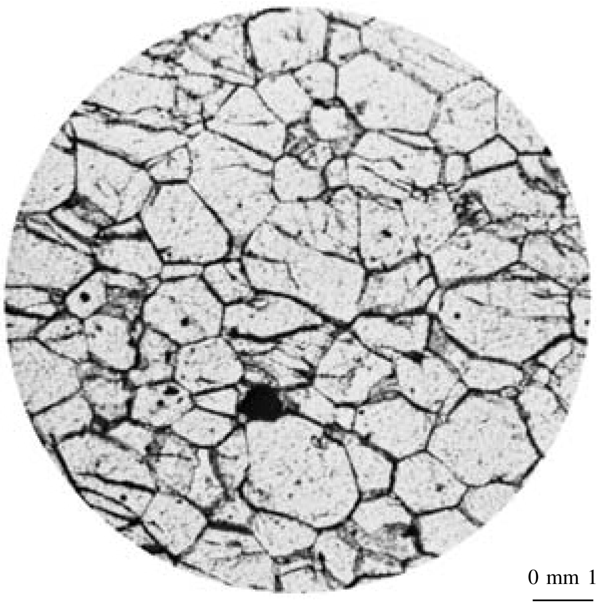

6.24 Dunite (olivine rock) under plane-polarized light showing ~120° grain boundary triple junctions. This texture reflects adjustment of grain boundaries to achieve minimal surface energy. Compare Figure 6.23. Black grain is a Cr-Al-Mg-Fe spinel.

clear evidence for homogeneous nucleation even for decompression-induced oversaturation, ΔP, as much as 130 MPa, equivalent to almost 6 km of ascent. However, they found that substantial *heterogeneous* nucleation occurred for ΔP as small as <1 MPa where minute Fe-Ti oxide grains served as bubble sites to overcome the kinetic barrier. Observed bubble densities were on the order of 10^6 bubble/cm^3 s. Bubble nucleation was slower on other minute "crystallites" of biotite, apatite, and zircon but required tens of megapascals of oversaturation. In apparently crystal-free melts, bubbles still appeared to be heterogeneously formed, perhaps on submicroscopic entities of unknown character.

Klug and Cashman (1994) found bubble "densities"—number of vesicles in a volume of natural silicic pumice—to be similar to those created heterogeneously in experiments and also noted greater vesicularity in glass that contains small crystals of crystals. Radial pipelike vesicles in basalt pillows and concentrations of vesicles in horizontal zones in the interiors of basalt flows may reflect bubble nucleation along crystallization fronts in these cooling magma bodies.

These experimental and empirical observations lend credence to heterogeneous bubble nucleation and indicate a link with crystallization.

Growth. A volatile fluid bubble in a static volume of melt adopts a spherical shape as a consequence of surface tension, which acts to minimize its surface area. Bubbles can grow to a diameter of as much as 10 m in low-viscosity basaltic magmas (Cashman and Mangan, 1994). However, most bubbles are much smaller, typically between a centimeter and a few micrometers, regardless of melt composition. Creation of a high density of bubbles in a melt produces, after solidification, a glassy silicic **pumice** or basaltic **scoria** in which the proportion of vesicle volume to whole rock is quite high. Corresponding bulk rock densities are low enough (several tenths of a gram per cubic centimeter) that pumice and scoria can float on water (density = 1 g/cm^3).

If bubbles are uniformly sized spheres, their theoretical maximum packing occupies 74% of the total volume; for nonuniform spheres the packing approaches 85%. Many natural pumices and scorias have vesicularities of 70–80%. In the very highly vesicular "thread-lace" basaltic scoria, also called *reticulite,* which has 95–98% voids (Figure 6.25), the vesicles are not perfect spheres but have a close-packed polyhedral shape (compare Figure 6.23) with only thin intervening filaments of glass. In silicic melts, the equilibrium bubble volume should be about 75% at depths of about 450–750 m and exceed 99% at 1 atm for common dissolved water contents of 4–6 wt.% (Klug and Cashman, 1996). Vesicularities upward of 93% are observed

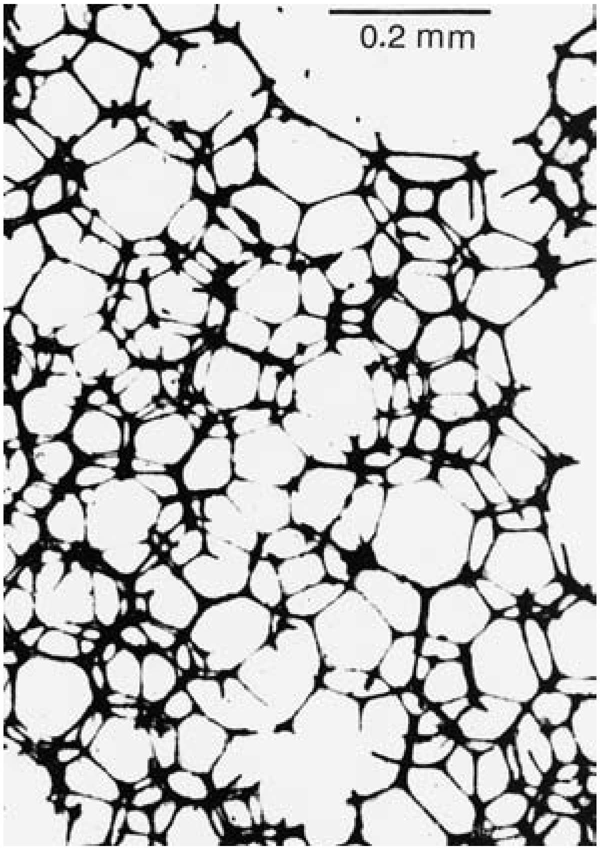

6.25 Thread-lace scoria (reticulite), Hawaii. Vesicle volume is about 98%. Compare Figure 6.23. (From Wentworth and Macdonald, 1953.)

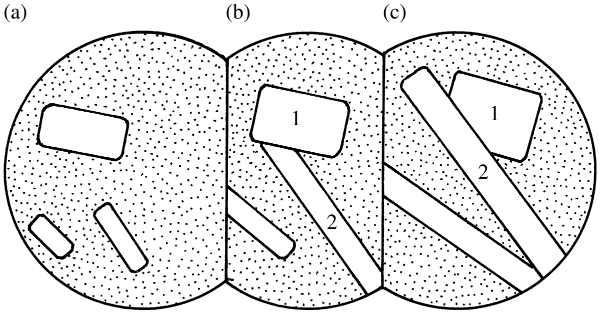

6.26 Grain-shape modification in coalesced grains. Tabular crystals of ammonium thiocyanate whose habit resembles that of plagioclase experienced modification of shape during cooling in a melt from 83°C–61°C over a little more than 3 hours. (a) Separately nucleated and growing crystals. (b) Growing crystal 2 impinges upon crystal 1. (c) The lower-energy, more stable large face of growing crystal 2 has encroached into what must be a higher energy and less stable face in crystal 1. The conventional textural interpretation of the common boundary of crystals 1 and 2 in (c) would be that crystal 1 grew against preexisting crystal 2, which in this case is incorrect. Diameter of fields of view is about 0.3 mm. (Redrawn from a photomicrograph in Means and Park, 1994.)

in fibrous pumice (Figure 6.27) in which vesicles are rod-shaped, probably as a result of stretching flow of the bubbly melt just prior to solidification. The optimal packing limit for rods, rather than spheres, is about 93%.

Many investigators have noticed a bimodal size distribution in vesicles in pumice—some are significantly larger than others, not unlike porphyritic texture for crystal sizes (see Figure 7.28b). Such a distribution could mean that some larger bubbles began to form before a nucleation "cascade" occurred during high oversaturation accompanying eruption that created many smaller bubbles. Alternatively, it may reflect coalescence of smaller bubbles to form larger ones.

Common silicic pumice has an overall surface area as much as 0.5 m^2/g corresponding to a sheet of glass 1 m^2 in area and only 0.87 micrometer thick (Whitham and Sparks, 1986). The energy expended in creating this surface area from an equidimensional volume of viscous melt is obviously considerable. (One may think of the work of rolling out a layer of much less viscous pie dough not nearly as large in area or as thin.) But this expenditure is only part of the total energy capacity in an exploding magma system. Additional energy is expended in breaking the pumice into pyroclasts and blasting them tens of kilometers against gravity into the atmosphere.

6.27 Fibrous, or woody, pumice lapilli in a pyroclastic deposit. Photomicrograph by scanning electron microscopy.

Growth of bubbles depends on several factors in addition to volumetric expansion of an existing volatile fluid in the bubble as the magma decompresses:

1. The melt viscosity that resists stretching of the bubble walls during volumetric expansion
2. Coalescence, or physical merging, of two or more bubbles into a larger one
3. Diffusion of volatiles through the melt walls to an existing bubble as intensive parameters continue to change, adding mass
4. Ostwald ripening, whereby small bubbles are consumed into larger ones by differential diffusion of volatiles through bubble walls (Mangan and Cashman, 1996)
5. Rate of magma ascent, or the rate of decompression and loss of heat
6. Volatile concentration and solubility

Which of these factors are most important in determining bubble growth in different magmas? Diffusivity depends strongly on viscosity, so this important parameter as well as concentrations of volatile species and solubilities must be considered. Rate of magma ascent also reflects magma supply rates and conduit attributes. Therefore, volatile concentration and solubility, ascent rate, and especially viscosity can be taken as the principal controlling factors in bubble growth.

One or more of these factors may be relevant in the contrast between nonexplosive extrusion of coherent magma, however bubbly it is, and explosive blasting of fragments of magma from a volcanic vent.

6.7.2 Melt Fragmentation and Explosive Volcanism

No one is really sure where, how, or why the transition takes place between a bubble-rich melt and an exploding magma. A common notion is that fragmentation occurs in a rising column of vesiculating magma (Figure 4.13) as the bubble volume exceeds a critical packing limit of 70–80%. However, the occurrence of unexploded pumice having higher vesicularity casts doubt on this notion (Gardner et al., 1996). A more fruitful line of inquiry may be to examine the three factors just enumerated, namely, volatile concentration and solubility and viscosity of the melt as well as magma ascent rate. Because viscosity may be the dominant factor, a comparison between the behavior of a low-viscosity basaltic magma and a highly viscous rhyolitic one might provide useful insights.

Explosive Basaltic Volcanism. Basaltic melts have not only low viscosity but high T so chemical diffusivities are large. Also, dissolved volatile concentrations, especially of water, tend to be lower than in silicic melts. A slowly ascending, decompressing, and cooling column of basaltic magma might experience near equilibrium bubble growth that keeps pace with changing intensive parameters. Larger bubbles might rise buoyantly through the magma fast enough to escape harmlessly from the top of the column. Exsolved volatiles may also be dissipated into openings in wall rock around the column. Variably degassed bubbly magma can erupt as coherent lava or in a mildly explosive manner.

More vigorous eruption occurs in basaltic **lava fountains,** which consist of molten blobs as large as bathtubs ejected hundreds of meters above the vent. Because of large bubble densities in fountain ejecta that imply large volatile oversaturation, Mangan and Cashman (1996) suggest that a rapidly ascending column of magma overshoots its saturation pressure and experiences a disequilibrium nucleation "runaway" and subsequent explosive degassing at less than about 100-m depth. The upward accelerating magma falls apart, much as water spray does in a high-speed fire hose.

Explosive Rhyolitic Volcanism. The dissolved water concentrations, commonly in the range of 3–6 wt.%, lower the viscosities of rhyolitic melts to only a few orders of magnitude more than basaltic. However, as a rhyolitic melt exsolves water into growing bubbles, the intervening melt walls between bubbles become drastically more viscous, impeding further bubble growth, both by restricting diffusion of more water into the bubble and by retarding viscous stretching of the bubble wall in response to volumetric expansion of the steam. Although increased viscosity would be expected to slow magma ascent, the increased volume of bubbles decreases the overall density of the magma, making it more buoyant and able to ascend faster. A high rate of magma ascent exacerbates the state of disequilibrium. Faster deformation of the magma during faster ascent in the volcanic conduit might cause the viscous melt to exceed its characteristic relaxation time (Section 6.1) so that bubble walls are, in effect, glass and the excess internal fluid pressure in the bubbles ruptures the walls. The result is explosive fragmentation of the magma.

A typical and important attribute of explosive rhyolitic deposits is the presence of a range of fragment sizes—ash, lapilli, and local blocks (Section 2.4.1). Ash is composed mostly, if not entirely, of glass shards that are largely ruptured bubble walls, whereas lapilli and blocks are composed mostly of unexploded pumice. Why is it that not every bubble in the exploding melt bursts? One possible reason for this heterogeneity in fragmentation (Gardner et al., 1996; Klug and Cashman, 1996) may be different degrees of bubble coalescence possibly resulting from uneven partitioning of strain in the melt during shearing flow accompanying rapid ascent and eruption from the volcanic conduit. Flow is indicated by widespread elongate, rod-shaped vesicles in pumice fragments (Figure 6.27).

Laboratory experiments have revealed fresh insights into explosive processes (Mader et al., 1994; Sugioka and Bursik, 1995). Test cells that contained CO_2 dissolved in HCl-K_2CO_3 solutions to mimic a volatile-rich silicate melt were monitored by high-speed photography. During decompression of the test-cell system, bubbles rapidly nucleated uniformly throughout the solution over a diffuse region, rather than at a well-defined, downward-propagating disruption surface. The expanding foam fragments heterogeneously where the bubble density and expansion rate conspire to rupture bubble walls.

SUMMARY

A change from some initial metastable state to a final more stable state is never instantaneous because it depends on time-dependent kinetic factors. The kinetic path between initial and final states of a melt depends, ultimately, on the mobility of ions. Melt viscosity and diffusion of ions are the two most important ionic transport phenomena because their time-dependent rates range over many orders of magnitude.

Melt viscosity is a measure of the resistance to flow, which depends on the mobility of atoms in it. Viscosity is less at high *T* because of the loosened atomic structure and in less polymerized melts that have less silica and/or more dissolved water and fluorine. Viscous melts have large relaxation times so that rapid deformation may cause them to break as if they were solid.

Atomic diffusion is net migration down a concentration gradient via random jumps. Diffusion is enhanced at high *T* and is generally fastest in gases, less in melts, and slowest in crystals. Large and highly charged ions diffuse slowly through more viscous melts, on the order of a few meters in 1 million years. Diffusion through crystals depends on the existence of point defects. The slowest diffusion involves exchange of Na^+Si^{4+} for $Ca^{2+}Al^{3+}$ in plagioclases even at high magmatic temperatures, preserving fine-scale (micrometer) compositional zoning indefinitely.

Thermal diffusivities are generally several orders of magnitude faster than chemical diffusivities. Consequently, static, nonconvecting bodies of melt cool and solidify before atoms can migrate more than a meter or so.

Crystallization is a two-step kinetic process that begins by formation of a nucleus and follows by accretion of ions onto it (crystal growth). Homogeneous nucleation requires significant undercooling so that the increasing difference between the free energies of the crystal and melt overcomes the surface energy contribution. Heterogeneous nucleation on various sorts of preexisting surfaces—solid and fluid—in the melt largely bypasses the kinetic barrier and could be the rule rather than the exception in magmatic systems. Shapes of crystals growing freely in melts depend on the degree of undercooling (cooling rate). Euhedral crystals having characteristic faces grow just below their liquidus *T,* but with increasing undercooling, crystals become less compact and are skeletal, then dendritic and feathery, and finally spherulitic for hundreds of degrees undercooling. If crystals grow faster than rates of diffusion, a compositional boundary layer develops at the crystal-melt interface.

Grain size in magmatic rocks is a compound function of nucleation and crystal growth rates. For similar growth rates, high nucleation density (integrated nucleation rate) yields small grains and low nucleation density large grains. A hierarchy in ease of nucleation depends on mineral structure and solubility in melts; among rock-forming minerals, Fe-Ti oxides nucleate readily and form small grain-size populations, mafic silicates nucleate somewhat more slowly, and commonly sluggish nucleation of felsic minerals, especially alkali feldspar, creates larger crystals.

Primary grain sizes can be increased (Ostwald ripening) and grain shapes modified because of the tendency for minimization of surface free energy.

Like crystallization, vesiculation is a kinetic phenomenon controlled by nucleation and growth of volatile bubbles in melts. Bubble nucleation, at least in silicic melts, appears to occur heterogeneously on minute crystals (crystallites). Bubble growth depends mostly on volatile concentration and solubility, ascent rate of magma in the crust, and, especially, viscosity. Low-viscosity basalt magmas are usually extruded as somewhat bubbly lava flows because vesiculation keeps pace with the rate of ascent in the conduit. Mildly explosive lava fountaining occurs locally, apparently as a result of rapid ascent and delayed catastrophic nucleation and growth of bubbles. Greater departure from equilibrium occurs during vesiculation of rhyolitic melts, especially during rapid ascent, because of their much greater viscosity, which increases as volatiles exsolve into bubbles. Exactly how factors such as excessive internal gas pressure in bubbles, viscosity and strength of bubble walls, melt relaxation time, bubble concentration, and shear flow during eruption interact to produce explosive volcanism has yet to be fully elucidated.

CRITICAL THINKING QUESTIONS

6.1 Contrast and characterize the three time-dependent transport phenomena with regard to mechanisms at the atomic scale, governing equations, driving forces, and proportionality constants.

6.2 Characterize and account for the viscosity of melts in terms of their composition, *T, P,* and concentration of dissolved volatiles.

6.3 List and discuss factors that govern the rate of diffusion of ions through liquids and solids.

6.4 Describe the role of diffusion in petrologic processes and how a knowledge of diffusion rates can provide insight into rock-forming phenomena.

6.5 Account for the large contrast in rates of chemical and thermal diffusion.

6.6 Discuss the nature of a phase interface and the importance of surface free energy in the kinetic paths and textural equilibria that influence rock fabric.

6.7 Contrast homogeneous and heterogeneous nucleation.

6.8 Describe a homogeneous nucleation model for a one-component melt and indicate limitations in applying this model to natural multicomponent melts.

6.9 Comment on the apparent relative nucleation rates of olivine, pyroxene, and plagioclase in the Makaopuhi basalt (Plate III), assuming growth rates are uniform.

6.10 Describe factors that control the growth and dissolution of crystals in a melt.

6.11 Discuss factors that govern grain size in magmatic rocks; grain shape.

6.12 What similarities and contrasts exist between nucleation and growth of bubbles and crystals?

6.13 Describe possible kinetic controls on fragmentation of melts and explosive volcanism.

6.14 What kinetic factors might be responsible for the highly explosive eruptions of some silicic magmas?

PROBLEMS

6.1 From Figure 6.2: (a) Plot viscosities, extrapolated if necessary, at 1100°C versus weight percentage silica for dry silicate melts. Explain your plot relative to the chemical composition of the melts and their atomic structure. (b) Plot viscosities of rhyolite melts with 77 wt.% silica at 800°C versus dissolved water concentration. Explain the drastic decrease in viscosity in the first 2 wt.% or so of dissolved water, followed by a lesser effect at higher water concentrations. How does the speciation of dissolved water, as $(OH)^-$ or as molecular H_2O, enter into your explanation?

6.2 Calculate the viscosity of Makaopuhi basalt melt at 1200°C using the chemical composition listed in Table 5.1 and the Shaw equation in Advanced Topic Box 6.1. How does your answer compare with the viscosity of $10^{1.51}$ Pa s measured experimentally by Shaw (1969)?

6.3 Calculate the activation energy of diffusion of O_2 through anorthite crystals (Figure 6.4).

6.4 Compare the diffusivities of water, H_2, and O_2 in a basalt melt at 1200°C. Calculate the average diffusion distance for these three species over 1 day. Could this have any bearing on the common red color of basaltic lapilli around explosive vents? Explain.

6.5 Freer (1981) cites $D = 9.66 \times 10^{-16}$ m^2/s at 1373K (=1100°C) for interdiffusion of Fe and Mg in Mg-rich olivine. Calculate the order of time to homogenize a compositionally zoned olivine crystal whose radius is 2 mm.

6.6 Demonstrate graphically that the ratio of surface area to volume, $4\pi r^2/(4/3)\pi r^3$, for spheres increases rapidly as the radius, r, diminishes to submillimeter dimensions. (*Suggestion:* Plot select values of r from 0.0002 to 0.015 mm against corresponding values of the ratio.)

6.7 Draw hypothetical homogeneous nucleation and crystal growth rate curves for a single mineral as a function of undercooling, and use these to illustrate the contrasts in the kinetic paths of glassy, aphanitic, and phaneritic textures.